A Microfacies Analysis of Arid Continental Carbonates from the Cedar Mesa Sandstone Formation, Utah, USA.

Ross P. Pettigrew*, Steven L. Rogers, Stuart M. Clarke

Basin Dynamics Research Group, Keele University, Keele, Staffordshire, UK, ST5 5BG.

*r.p.pettigrew@keele.ac.uk

Abstract

Arid continental environments are typically dominated by siliciclastic aeolian, alluvial and fluvial deposits. Despite their common recognition within these environments, carbonate deposits are often overlooked, yet they can provide vital insight into the depositional history, climate, and tectonic controls of a sedimentary basin. This work presents a detailed microfacies analysis of the carbonates found within the Cedar Mesa Sandstone Formation of the Western USA. The Cedar Mesa Sandstone Formation is an early Permian, predominantly aeolian succession, exposed across much of the Colorado Plateau of southern Utah and northern Arizona. The formation is dominantly clastic erg deposits, that grade into a mixed carbonate/clastic sedimentary succession interbedded with carbonate and evaporitic units, interpreted to represent sabkha or sabkha-like deposits. Whilst many authors have worked within the aeolian dominated facies and have proposed various facies schemes for the siliciclastic components, comparatively little attention has been paid to the mixed evaporitic/clastic/carbonate aeolian-sabkha transition zone. In this work the microfacies of the carbonates present within the Cedar Mesa Sandstone are analysed, in order to: (i) develop a record of, and interpret carbonate components, (ii) propose depositional mechanisms and (iii) identify evolutionary trends that stand alongside the formation’s clastic depositional story. Six microfacies are presented: MF1) Clastic Influenced Carbonate Wackestone; MF2) Laminated Carbonate Wackestone/Packstone; MF3) Microbial Laminated Fenestral Bindstone; MF4) Rounded Mudclast Wackestone; MF5) Laminated Bioclastic-Ostracod-Carbonate Wackestone and MF6)

Microcrystalline Quartz. The microfacies have been interpreted to document the development of carbonate interdune, lacustrine and continental sabkha environments influenced by localised fault control juxtaposed across a wetting and drying climate cycle and provide useful comparisons for other mixed evaporite/carbonate and clastic sequences.

Keywords: Continental Sabkha, Microbial Carbonates, Microfacies, Utah.

Introduction & Geological Setting

Carbonates, although less common than aeolian, alluvial and fluvial deposits, feature in many arid continental settings, and have been recognised widely within both modern and ancient (Dorney *et al.*, 2017; Sanz *et. al.*, 1995) deposits. They form through complex interactions between ground waters and soils (Spötl & Wright, 1992) within interdune or desert-lacustrine settings (Platt, 1989; Driese, 1985; Seard *et al.*, 2013; Parrish *et al.*, 2017), springs and tufa mounds (Dorney *et al.*, 2017), or from marine incursions (Jordan & Mountney, 2010, 2012). Despite being recognised frequently, carbonate deposits within arid continental basins are rarely studied in detail (Mountney & Jagger, 2004; Langford & Chan, 1988, 1989; Moutney, 2012). This apparent ‘sedimentary bias’ is unfavourable as carbonates can provide vital insight into the depositional history, palaeoenvironmental ecology, climatic and/or tectonic controls of a basin (May et al., 1999; Rogers, 2018).

The predominantly aeolian successions of the Cedar Mesa Sandstone Formation are exposed across much of the Colorado Plateau of southern Utah and northern Arizona, and they represent an early Permian, northeast-southwest trending desert system bounded by a palaeoshoreline to the northwest (Blakey, 1988; Blakey *et al.*, 1988; Huntoon *et al*., 2000, Fig. 1). In the southeast corner of present day Utah, the Cedar Mesa erg deposits grade into mixed evaporite/carbonate and clastic sediments that are interpreted as sabkha deposits of an erg-marginal transition zone (Huntoon *et al*., 2000; Condon, 1997: Blakey, 1988).

Whilst many authors have worked within the aeolian erg-dominant facies of the Cedar Mesa Sandstone Formation and have proposed various facies schemes for the siliciclastic components

(Mountney 2006; Mountney & Jagger, 2004; Loope, 1984), comparatively little attention has been paid to the mixed evaporitic/carbonate and clastic erg-marginal transition zone (Langford & Massad , 2014).

This work presents the first petrographic study of the carbonates found within the erg-marginal Cedar Mesa Sandstone Formation. The study area is located west of the town of Bluff, Utah (Fig.1), where the Permian sediments of the Cutler Group are well exposed within east-west orientated incised canyons. 10 sedimentary logs through the erg-marginal transition zone of the Cedar Mesa Sandstone Formation were recorded. Each log extends from the underlying lower Cutler beds (see Jordan & Mountney, 2010) to the overlying Organ Rock Formation (see Cain & Mountney, 2009).

The study area lies between two antithetic extensional faults (Fig. 1), representing inherited Precambrian basement structures with multiple phases of movement (Davis, 1999), but present today as the Comb Ridge and Raplee Ridge monoclines (Fig. 1) as a result of Laramide structural inversion (Mynatt *et al.*, 2009; Hilley *et al.*, 2010; Kelley 1955: Davis, 1999; Huntoon, 1993). A depositional mechanism driven by periodic marine incursions has been suggested by Stanesco & Campbell (1989) based on isotopic analysis. However this interpretation is based on a few data points generated from materials susceptible to recycling of marine signatures (*cf.* Taberner *et al.*, 2000), and analyses of the clastic component of the Cedar Mesa Sandstone Formation (Mountney, 2006; Langford & Massad , 2014) suggest a wholly-continental formation mechanism for these deposits driven by cyclic climate variations.

Analysis of the carbonate units within the sabkha-like sediments of the Cedar Mesa Sandstone Formation and presented here: 1) provides a detailed microfacies analysis of the carbonates present within the Cedar Mesa Sandstone Formation, in order to develop an understanding of the carbonate components; 2) identifies the features indicative of particular depositional constraints; 3) builds depositional models which explain the presence of the carbonate deposits and contribute to the understanding of the Cedar Mesa Sandstone Formation. Subsequently this work provides insight into the role in which inherited structure and climatic variations can affect the sedimentology, and provides a comparison between mixed evaporite/carbonate and clastic sequences from wholly continental arid successions and those with a marine influence such as the Permian Zechstein of Northern Europe.

Methodology

Sedimentary logs were recorded at approximately 3 km intervals from north to south through the study area using east-west orientated canyons which cut perpendicularly to the general north-south strike of the strata. The sedimentary logs cover 30–150 m of succession, with the carbonates appearing sporadically throughout six of the logged sections (Logs 1.2, 1.3, 1.4, 1.5, 1.7, 1.8) (Fig. 1).

The carbonates are interbedded between thick successions (up to 10 m) of either aeolian, fluvial/lacustrine derived sandstones, or evaporites. Samples were collected from the middle of each available carbonate unit, or from the top and bottom of the unit where thicker deposits (40-50 cm) allowed. This resulted in 65 samples (rock samples and thin sections) collected from the log localities (Fig. 1). 30 μm thick, unstained, thin sections were produced from each sample and subsequently investigated using a Nikon Eclipse LV100N POL microscope, at Keele University, UK. The microfacies of the carbonate units were analysed and classified following the modified Dunham (1962) scheme of Lokier & Al Junaibi (2016), with the percentage of clastic components calculated using comparison charts. Five microfacies and one diagenetic alteration texture have been identified and are presented here. For continuity and ease of reading the diagenetic alteration texture is referred to as a microfacies, although we acknowledge that this is against the standard definition of a microfacies.

Results

In the field, carbonates of the Cedar Mesa Sandstone Formation are generally dark grey to blue, and appear homogenous. Individual carbonate units are generally 20–50 cm in thickness and present as either isolated lenses up to 3 m in width (Fig. 2B, Fig. 2F) or laterally continuous units over 10’s of metres Fig. 2C, Fig. 2E). Outcrop specimens with a wavy–laminated (Fig. 2A) or nodular texture (Fig.

2D) are classified as a wackestone, however, some sand-grade-grain supported carbonates are classified as packstones (Fig. 2BandF). The carbonates sporadically appear interbedded with gypsum (Fig. 2D) or with chert nodules, but weather to form predominantly blocky units in outcrop (Fig. 2B and E) between 20–40 cm thick.

MF1: Clastic Influenced Carbonate Wackestone

This facies crops out as isolated, dark grey to blue, siliciclastic, massive fine-grained wackestone (Fig. 2B). The microfacies has a high clastic component (approx. 10–>50%) within a darker, homogenous dark brown carbonate mud matrix. Some specimens show poorly defined wavy laminations (Fig. 3A), but otherwise most examples lack any sedimentary structures. The carbonate mud matrix is composed of micrite with sparse microspar crystals. There are occasional isolated rounded intraclasts of mudstone with a higher microspar component that float within, and appear slightly lighter than, the background quartz-micrite-rich matrix (Fig. 3B and C). Quartz grains are dominantly well-rounded to sub-rounded, well sorted and fine to medium-grained (Fig. 3A, through C). The majority of intraclasts have sporadic calcified tube-like structures, clotted micrite textures, and are found in association with micrite envelopes. A thrombolytic texture is sometimes preserved, where darker micrite appears to have enveloped “cauliflower”-like structures (Fig. 3C).

MF2: Laminated Carbonate Wackestone/Packstone

MF2 is a siliciclastic-rich (10–40% sand grains), dark grey to blue, fine-grained wackestone- to packstone, found as horizontally and laterally restricted lenses, approximately 2 m in width. The microfacies is characterised by bedding-parallel laminations of dark-brown carbonate mudstone matrix, alternating with either laminations of quartz grains or undulose laminations of light-brown to grey clotted microbial fabrics (Fig. 4A and B). Clotted micrites are typically thrombolytic with peloidal and some protostromate features (calcified tubes) present. Quartz grains are moderately sorted and have a rounded to sub-rounded texture (Fig. 4C). Ostracods occurrences are infrequent (less than 1% of the microfacies) and randomly distributed (Fig. 4B), but otherwise the microfacies is barren of metazoan skeletal grains.

In one sample, horizontal laminations (0.5–0.8 mm thick) of fine-grained quartz grains alternating with a thinner (0.1–0.2 mm), flat-to undulose, brown carbonate-mud matrix were observed. The laminations of quartz grains show slight normal grading from medium to fine grained (Fig. 4C). The laminar fabric is supported by the sand-grade grains (which are considered as extraclasts within the carbonate) resulting in a packstone classification.

MF3: Microbial Laminated Fenestral Bindstone

This facies crops out over laterally continuous distances between 5–10 metres as a dark-grey to blue-grey, laminated, lime-bindstone. Beds of MF3 measure between 20–40 cm in thickness and are enclosed primarily between evaporitic gypsum deposits (up to 5 m thick), as well as wave-rippled sandstones and palaeosols (0.5–2 m thick). The microfacies can be subdivided, MF3a is characterised by a dominant laminoid fenestral (LF) fabric, consisting predominantly of type LF-A (horizontally linked lateral fenestral fabrics), but with some isolated areas of type LF B-II (horizontal cavities with laminoid fabrics) with elongate fenestrae and strings of regularly spaced birdseye-like voids between laminated, peloidal and oncoidal clotted fabrics. MF3b is characterised by thinner and more irregular fenestrae within laminated micrites that typically show an undulose habit. See Tebbutt *et al*., (1965) and Müller-Jungbluth & Toschek, (1969) for further information on laminoid fenestral fabrics.

The MF3a is characterised by fenestrae that are arranged concordantly to the stratification. The dominant fabric consists of elongate fenestrae (Fig. 5A) which sit parallel to local contortions within the grain-supported sediment (LF-A). In places these fenestrae appear as strings or chains of regularly spaced birdseye-like voids (approximately 30 μm in diameter) (LF-BII) (Fig. 5A). Both of these void types appear morphologically related; the thickness of the voids are the same (30 μm), they regularly occupy similar positions in sections (e.g. sit along the same laminations) and both are frequently encrusted (possibly scaffolded) by laminated, cyanobacterial and/or microbial structures (Fig. 5B and C). In places, encrusting elements have been reasonably well preserved, with tube and chamber like structures observed (Fig. 5C and E). Encrusters are reminiscent of organisms such as *Rothpletzella* and *Girvanella* (Fig. 5E). The sedimentary framework of MF3 is dominated by oncoids and peloids (Fig 5D). Peloids occur as several microns to tens of microns wide mictite-grains that are often devoid of internal structures, however, there are examples where tubular and rounded calcified tube-like structures are present (Fig. 5D). The porostromate features are more prominent in the larger (up to 300 µm in diametre) oncoids (Fig. 5D), which typically display laminated features including similar tubular and rounded structures to those of the peloids. These grains are morphologically related (only differing in size), and are thus grouped here as oncoids. The oncoids are often found in association with LF B-II fabrics and can be observed as internal sediments to the voids in places (Fig. 5C).

The MF3b is characterised by laminated, 10–20 µm thick, undulose micrites conspicuous as alternating lighter and darker laminae, with elongate fenestrae (Fig.5A and E). These voids are both fewer in number and thinner (several to tens of microns), than their MF3a counterparts. The micrite laminations typically contain tube-, chamber-, sausage- and bean-shaped structures and form the lighter laminae. As in MF3a, these encrusting organisms resemble known encrusting forms like *Rothpletzella* (Fig. 5E).

Rounded lithic clasts (consisting of both carbonate and quartz grains) are found locally, exhibiting thin (20–30 µm) micritic envelopes consisting of tubular structures. They are observed more typically near to the boundary between the carbonate units and the underlying clastic sediments, with the tops the units devoid of clastic grains. Evaporite pseudomorphs and casts are observed sporadically throughout this microfacies.

MF4: Rounded Mudclast Wackestone

MF4 crops out as laterally continuous dark grey to blue mudstone to wackestone (Fig. 2). The matrix of this microfacies is a dark brown carbonate mud matrix. Rounded intraclasts of slightly lighter microspar mudstone are dispersed throughout (Fig. 6). The microfacies contains very few occurrences of bioclasts with only minor occurrences of ostracods (between 1–5% of the microfacies) irregularly distributed throughout the samples (Fig. 6C), though more abundantly than in MF2. Isolated quartz grains are sporadically distributed. The matrix is generally homogeneous although evidence of poorly defined clotted textures has been observed (Fig. 6C). The mud clasts are commonly ~1 mm in size with a few larger examples (up to 3 mm) present. The clasts account for up to 40% of the microfacies.

The surfaces of these clasts are often the nucleation point for stylolites found throughout this microfacies, with some clasts surrounded by the compressional fractures (Fig. 6A). The stylolites are typically oriented parallel to bedding and occur spaced sporadically throughout the samples.

MF5: Laminated Bioclastic-Ostracod-Carbonate Wackestone

This facies crops out as laterally continuous dark grey to blue coloured, fine-grained carbonate mudstone to wackestone (Fig. 2E). The microfacies is characterised by a brown, laminated carbonate mud with a clotted textured matrix. Interspersed laminations of microspar and some peloidal and clotted areas with lighter grey/green thrombolytic textures are also present. The thrombolytic textures typically consist of clumped and tangled protostromate features. Laminations or envelopes of micrite are typically associated with these tube-like structures. The bioclasts are dominantly composed of cross-sections through carapaces and individual valves of Podocopa ostracods (comprising up to 25% of the microfacies) alongside some larger isolated shell-like fragments (Fig. 7A). Complete ostracods are mostly aligned with bedding and are between 30–60 µm in length. Ostracod tests appear white and the broken skeletal grains show a dominant convex upwards arrangement along a bedding horizontal plane (Fig. 7C). Isolated fenestral cavities are present, particularly within the more micritic layers; several stromatictis-like cavities were observed (Fig. 7B and E), exhibiting flat, sediment-filled bases with an undulous cavity roof, a thin isopachous cement rim, and with later blocky calcite cement fill (Fig. 7E). There is some evidence for ‘wavy’ laminations (Fig. 7D), but much less frequently than in MF3. The microfacies is largely devoid of clastic grains, with minimal occurrences of isolated quartz grains.

MF6: Microcrystalline Quartz

This facies crops out as either isolated nodular bands of dark red chert or nodules. Samples are dominantly composed of microcrystalline quartz and show a variety of habits from microflamboyant quartz (cf. Milliken, 1979), to random fibrous granular microcrystalline quartz (Fig. 8A), and to rimmed, radial, and undulose megaquartz (Fig. 8B). Evaporite inclusions are typically present (Fig.

8C), and frequently show evidence for the displacement of the original carbonate material (Fig. 8D) in association with filled fractures of fibrous microquartz (Fig. 8C).

Spatial Distribution and Sedimentary Relationships

Key sedimentary relationships and the nature of the interbedded clastic deposits have been examined (Fig. 9) along with a schematic plot of the microfacies types against sample location within the sedimentary successions (Fig. 10). The sedimentary relationships indicate that certain microfacies are more commonly associated with different clastic sediments, and the positioning of the various microfacies sheds light on some of the local environmental conditions that it is not possible to glean from analysis of the siliciclastic sediments alone.

The MF1, with a total of 21 occurrences, is the most common microfacies. It occurs in relationship with aeolian clastic deposits, both laterally and stratigraphically. The clastics comprise primarily trough-cross-bedded, medium-grained, sandstone sets (Stxb) arranged into cosets (up to 10 m thick) and massive sandstone (Sm). Foresets of the cross-bedding display alternating grainflow and grainfall couplets indicating that the sediments are the product of migrating sinuous-crested aeolian duneform trains. Massive sandstone units (Sm) range between 0.2–1 m thick and comprise poorly defined wind-ripple strata with a limited grainsize range that results in a massive appearance. Rhizoliths, up to 1 m in length, are typical. They branch along horizontal planes (up to 50 cm in width) and fine to a point towards the base of the unit. In addition to these facies, MF1 occurs sporadically in relationship with units of wave-rippled sandstone (Swr), palaeosol (Sfo) or gypsum (G), all no greater than 0.5 m in thickness.

The MF2 shares similar sedimentary relationships with clastic facies to those of MF1. The facies is found typically in association with planar-cross-bedded sets of medium-grained sandstone (Sxb) that sporadically form cosets 1–5 m thick. Foresets of the cross-bedding display alternating grainflow and grainfall couplets indicating that the sediments are the product of migrating straight-crested aeolian duneform trains. Massive sandstone units (Sm), up to 1 m in thickness, are found typically in associations with MF2, as are wave-rippled (Swr) sandstones and palaeosols (Sfo), although in much higher frequency than for microfacies MF1. Low-angle, planar cross-bedded, 0.2–0.5 m thick sandstone sets with erosional bases (Sfxb), interpreted to be fluvial sheetflood deposits, are also present in association with this microfacies.

The MF3 occurs typically in stratigraphical and lateral association with gypsum deposits (G) or with gypsum-bound sandstone (Gspl). The gypsum deposits are characterised by multiple enterolithic growth structures and tepee structures, and the gypsum-bound sandstone comprises a pastel-blue fine-grained sandstone that is moderate to poorly-sorted and contains a gypsum-rich matrix and cement, often with multiple gypsum nodules distorting primary sedimentary textures. Palaeosol units (Sfo) and wave-ripple sandstone (Swr) units are also sporadically present in association with MF3.

The MF4 is deposited primarily in association with sheet flood deposits (Sfxb) or wave-rippled sandstones (Swr). The microfacies is also present in relationship with fining-upwards beds of structureless, dark-grey to black silts (Ssl) which range between 0.2–1 m in thickness.

The MF5 occurs almost exclusively in lateral and stratigraphic association with thick deposits (0.5–3 m) of fining-upward silts (Ssl), minor sheet-flood (Sfxb) or wave-ripple sandstones (Swr) deposits.

The MF6 has seemingly no stratigraphic or lateral association with a distinct set of coeval clastic deposits. As this ‘microfacies’ is not carbonate, and is probably the result of secondary alteration, its spatial relationship might suggest a non-discriminatory alteration process.

Interpretation & Palaeo-Environment

With the microfacies described, environmental interpretations are made for each of the five carbonate microfacies (MF1–MF5) and placed into context of the larger sedimentological framework of the Cedar Mesa Sandstone Formation.

MF1

The high content of detrital well-rounded and sorted quartz material indicates deposition occurred in close proximity to a relatively mature clastic sedimentary system. The carbonate mud matrix along with the occasional carbonate grains may represent many depositional environments, however, the close lateral and stratigraphic proximity to sub-aerial deposits (Stxb, Sm) probably indicates extremely shallow (few centimetres) quiet waters. The carbonate grains formed of micro-spar may originate from reworked carbonate material, potentially transported into the system with the clastic component (*cf.* Lokier *et al.*, 2017). The general lack of evaporites or of any desiccation structures in association with this microfacies suggests sufficient water to maintain long-standing pools/puddles of water suitable for carbonate development. The lack of bioclasts, along with lensoidal geometries suggest an isolated depositional setting (Driese, 1985), lacking input from, or connectivity with larger bodies of water.

MF2

The sedimentary framework of alternating laminations of fining upward, sub-rounded moderately-sorted quartz and clotted micrite fabrics within a more homogenous carbonate mudstone matrix indicates periodic influxes of clastic material, followed by a hiatus in the input of detrital material. This resulted in clotted micrite carbonate precipitation, most likely mediated by microbial communities, as evidenced by the protostromate remains and structures that are most likely to be *Rothpletzella* and *Girvanella*.

Normal grading of moderately sorted quartz shows suspension settling of clastic sediment from a more immature detrital source than indicated for MF1. Isolated and lens-shaped geometries indicate a restricted setting. Rare occurrences of skeletal grains (ostracods) could suggest periodic connection to wider environments. However, the scarceness and random distribution of skeletal grains could favour wind-blown dispersal (Chaplin & Ayre, 1997).

The presence of clotted and laminar microbial growth also indicate an environment that was wetter than that for MF1. The features are similar to those observed from stromatolites (see Warke *et al.,* 2019) which form under conditions generally, deeper, and longer-lived standing water than features observed within MF1.

The high clastic content of MF1 and MF2, and their stratigraphical relationships to coeval aeolian clastic deposits (Fig. 9), suggest deposition within wet interdune areas. Wet interdunes form when there is a perennial water table in contact with, or above, the depositional surface to form ponds and lakes between dunes (Ahlbrandt & Fryberger, 1981). These long-lived ponds can feature, as observed here, wave-rippled and laminated siltstones, as well as evaporites and carbonates (see Mettraux *et al*., 2011 for an example of modern equivalents). Wet interdunes have, or exhibit, a variety of morphologies, which are controlled by the shape and style of migration of the aeolian dunes. Highly sinuous dunes result in isolated interdunes with limited lateral extent, whereas straight-crested dunes may develop and preserve large corridors of laterally continuous interdune. The shape and style of dunes, and therefore interdunes, is highly reliant on climate and sediment supply and availability (Mountney, 2006; Rubin, 1987; Rubin & Carter, 2006). The deposits of MF1 are the most abundant microfacies observed, however, field observations indicate that they are limited in lateral extent (<1 m) and occur typically in close proximity, both laterally and stratigraphically, to aeolian dunes. The high clastic content, limited lateral extents, lack of skeletal metazoan clasts, and occurrences of relatively few microbial mediated carbonates indicate a depositional environment typical of the restricted and isolated setting of wet interdune areas between sinuous-crested migrating dunes. Evidence for such duneforms is reported here, and within the formation by previous authors (Langford & Massad, 2014; Mountney & Jagger, 2004). The clastic sediment observed within the microfacies is supplied by wind action from the nearby dunes (*cf.* Driese, 1985). The relative high abundance of MF1 may be related to a high preservation potential as interdune areas were eventually covered and preserved by migrating dune complexes (Driese, 1985).

MF2 shares a similar clastic content to that of MF1. However, clotted and laminar microbial growth is present and clastic sediment is more angular and more poorly sorted. Detrital clastic material occurs in regular bands of fining upwards material, with occasional ostracods present. Interbedded bands of clastic sediment indicate periodic influxes of detrital sediment or localised reworking, suggesting larger interdune bodies with significant periods of interconnectivity between them, and possibly with connection to wider environments. An increased lateral continuity in outcrop of MF2 (compared to MF1), coupled with associations with clastic deposits of straight-crested migrating duneforms, supports an argument for larger, better-connected interdunes (Fig. 11). These settings are typically associated with periods of limited aeolian sediment supply, such as those found on the very edge of the erg, or those typical of higher water tables during humid periods, where clastic input to interdune areas is from fluvial influx, and sediment can be reworked (Mountney, 2006; Howell & Mountney, 1997).

MF3

MF3 is rarely preserved within the study area, but where present MF3 is laterally extensive and often in association with evaporites. The sedimentary framework of this microfacies is dominantly micrite exhibiting pelloidal or oncoidal features (MF3a) with common evidence of laminar, encrusting modes of formation either within grains or as laterally persistent laminations (MF3b). These grains are interpreted to be benthic peloids and oncoids, forming from similar mechanisms and processes (i.e. biochemical precipitation triggered by microbial activity), but growing to various sizes. The encrusting nature of the laminar structures indicates that these are primary grains, rather than reworked components (e.g. MF3b). The laterally continuous laminations of MF3b are interpreted to be algal and microbial mats, similar to those observed in modern day Abu Dhabi (Court *et al*., 2017). Undulations observed for these laminated components appear to be primary; there are no microstructures present to indicate secondary compression and the orientation of individual laminations can be seen to be columnar, bulbous and wavy in places (Fig.5B).

Fenestrae in this microfacies are interpreted as primary cavity networks. Sediments within cavities indicate that the cavities were part of a network through which currents were flowing at the time of primary deposition. The elongate voids common to MF3a are often sheathed in microbial structures. These are related to the primary construction of the voids, as the chain-like cavities often display the same sheath like envelope. These encrusting features then join from the base and roof of the voids to form column-like structures that appear preserved as rows of spaced birdseye-like voids. Encrusting forms such as *Rothpletzella* and *Girvanella* have been observed to act as constructors of cavities in other microbially dominated carbonates (Rogers, 2018). Laminations and laminoid fenestrae indicate shallow-water to sub-aerial exposure, and they are often used as indicators of sea level. However, Bain & Kindler (1994) demonstrated that fenestrae should only be associated with sea-level where other features associated with intertidal- or peritidal characteristics exist. Here, no further evidence for tidal influence is found. Birdseye cavities also generally occur in shallow (intertidal) marine, lacustrine and even in eolianite environments where rainwater induces cavities (Bain & Kindler, 1994). Shinn (1968) reported that birdseye cavities never form in the subtidal zone. It is therefore likely that MF3 was deposited in extremely shallow water and the sediments typically experienced a certain amount of subaerial exposure. The cavities may have formed as desiccation-related structures that were subsequently colonised by encrusting cyanobacteria, resulting in their preservation. The lack of skeletal metazoan grains suggests restricted depositional environmental conditions that were inadequate, or too stressed for other biota.

These most likely represent the deposits of laminated microbial mats (Lokier *et al*., 2017; Riding, 2000; Van Gemerden, 1993). Microbial mats are present in many environments, however the spatial relationships seen here indicate a likely evaporitic depositional setting, either a marginal marine, or continental sabkha. Marginal marine sabkhas are characterised by pelodial and bioclastic carbonates within the lower intertidal zones, microbial mats within the middle to upper intertidal zone, and evaporites mixed with clastic deposits within the supratidal zones as demonstrated by Court et al. (2017) in the Abu Dhabi Marine Sabkha. Continental sabkhas, such as those interpreted here, share many of these key features, however, the formation mechanisms are different. Saline pans form evaporites from the desiccation of desert lakes which are subsequently sub-aerially exposed as crusts mixed with clastic sediment derived from the suspension and settlement of floodwaters (Lowenstein & Hardie, 1985). Variations in saline ground waters promote phreatic growth of evaporite crystals and nodules around these salt pans forming saline mudflats (Lowenstein & Hardie, 1985; Warren, 1983). These saline mudflats are a recognized habitat for microbial life in desert environments as the interaction between the salt flat and the groundwater provides sheltered habitats for microbial life (McKay *et al.*, 2016).

MF3 shows abundant evidence of shallow, restricted deposition. Undulous laminations associated with laminoid fenestrae are common and microbial mediation of micrite can be interpreted from the peloidal, thrombolytic and protostromate features observed. MF3 is therefore interpreted to belong to a shoreline of a continental playa-lake environment.

Microbial mats typically have a very low preservation potential (Court *et al.,* 2017) and are regularly destroyed within marginal marine settings by tidal processes and storm events, preservation therefore favours low energy environments. This further indicates that the microfacies likely formed within a continental sabkha setting rather than a marginal marine setting, around the edges of low energy saline lakes, increasing preservation potential. The presence of coeval lacustrine clastic sediments, and the framework of a continental playa-lake discussed by other authors (Langford & Massad, 2015) also support this argument. The distorted and fensetral form of the microfacies suggests lateral growth (Lokier *et al.,* 2017*;* Court *et al.,* 2017), loading and degassing. This could be driven by the encroachment of aeolian dunes, which would enhance preservation potential (as seen within MF1) during an arid climate (*cf.* Kocurek, 1981; Driese 1985).

MF4

The rounded mud clasts within this microfacies have similar features (laminated micrites, protostromate features) to some of the other microfacies described here (particularly MF3 and MF5). It is suggested that these clasts may be reworked from partially lithified sediments from the proximal sedimentary environment. The reworking of this deposited material was coeval with the deposition of this sediment. The mudstone clasts composed of microspar grains may indicate reworking of a feature where carbonate sands may be present. The rounding of the clasts indicates transportation of the grains. The lack of sediment lamination and the absence of cavities suggests that this microfacies occurred in water that was deeper than microfacies MF1, 2 and 3. The lack of laminar cavities is interpreted to indicate a lack of primary microbial mats and puckering/desiccation associated with sub-aerial exposure. The lack of Birds-eye cavities suggests that the microfacies was deposited in a setting permanently below the surface of the water. Ostracod occurrences, although in low numbers, are more frequent than the previously described microfacies (ostracods were absent from MF1 & 3). This may indicate a slightly less restricted or isolated depositional environment than those interpreted for MF 1, 2 and 3. Stylolites within this microfacies are not associated with primary tectonism, they are not regularly spaced and are oriented parallel to bedding, indicating they formed due to loading due to an applied sedimentary load and burial. MF4 lacks laminations and is homogeneous in appearance, with the exception of rounded mud clasts, this is interpreted to represent an environment which was deeper, or more persistent than those previously described (ostracods within these sediments also indicate larger, possibly better connected or more pervasive water). The rounded mud clasts, which have some shared features with the microfacies interpreted to be from extremely shallow environments (e.g. MF3) were likely transported from these shallower areas, possibly similar to the transport of sediment in sabkha environments through higher-energy events as described by Lokier *et al*. (2017). The common stratigraphic association of MF4 with fluvial deposits (Sfxb) likely provided the transport mechanism for the reworking of clasts (Fig. 9).

MF5

The sedimentary framework of this microfacies is dominantly micrite with few microbially encrusted laminations or cavities present. The microfacies is similar in appearance to MF4. Relatively abundant ostracods are present indicating a less restricted environment than the microfacies previously described, indicating deeper water and/or better connected (less restricted) water bodies. Cavities are interpreted to be the result of gas bubbles (or to have a biological origin) rather than desiccation (and subsequent encrusting biota construction) related, this may explain why they are less frequent than in

MF3. The presence of stromatactis-like cavities is not indicative of any one setting as the formation mechanism of the cavities is still somewhat enigmatic (Monty, 1995; Aubrecht *et al.,* 2002; Hladil, 2005). Two main hypotheses exists suggesting either a purely biological origin (Tsien, 1985; Flajs & Hüssner, 1993) caused by the collapse (Bourque & Gignac, 1983) or syndiagentic shrinkage of sponge bodies (Delecat & Reitner, 2005) with the coexistence of stromatactis in sediments with bioclastic sand, large oncoids, and calcareous algae indicative of shallow-marine environments (Stenzel and James 1995). Alternatively a physical origin has been proposed (Wallace, 1987; Kukal, 1971) for stromatactis cavities, due to filling of cavity systems with cement and sediment (Bathurst, 1980) or formation during turbulent deposition and separation of unsorted clastic material within dispersed suspension clouds (Hladil, 2005, Hladil *et al.,* 2007, 2006). However, the presence of stromatactis-like cavities does indicate that the depositional environment was quiet and sub-aqueous.

The low diversity, but high productivity of the microfacies suggests a restricted environment, and it is likely that salinity played a restrictive role. This high salinity, restricted environment and lack of body fossils would make the formation of these stromatactis-like cavities by sponges seem unlikely,. The laminated nature of the microfacies with disarticulated ostracods along bedding planes, could indicate periodic reworking and detrital input into standing bodies of water during higher energy events, creating turbulent conditions and subsequent settlement, resulting in bedding plane parallel ostracods and turbulent flow generated stromatactis-like cavities (*cf.* Hladil, 2005, Hladil *et al.*, 2006, 2007). The common association with lacustrine suspension-settle deposits (Ssl) further supports this argument, with turbulent flows created from the input of fluvial deposits (Sfxb) (Fig. 9).

Bioclasts and ostracods are abundant only in MF5 with rare or sporadic occurrences within MF2 and MF4. The microfacies are laminated to varying degrees, except MF4; which has clear evidence of reworking of grains. MF4 and 5 are both interpreted to belong to a desert lacustrine system.

MF5 shows a lot of features similar to MF3 however the microbial mats are broken up and disjointed indicating remobilisation and modification of sediments from previously deposited mats. This is possibly related to the flooding of these saline lake edges due to lake contraction and expansion related to shifting environmental controls (i.e. arid and humid periods, see Mountney, 2006). The layered appearance of MF5 indicates deposition formed by suspension settling within calm long standing bodies of water, with occasional turbulent conditions generating stromatactis-like cavities. The abundance of ostracods and larger shelly fragments (Fig. 7D) indicate conditions more conducive to bio-productivity than the previously described microfacies and could indicate lower salinity levels. MF5 most likely represents deposition within long lived desert lacustrine systems (Fig. 11). Stromatactis-like cavities indicate there was no sub-aerial exposure. Desert lakes, often related to topographic lows, frequently deposit parallel laminated and ripple laminated silts and mudstones from suspension settlement, as well as fresh water carbonates, when the availability of clay-size particles is limited, primarily as a result in climatic fluctuations (Tanner & Lucas, 2007). Deposition likely occurred within deeper parts of lakes away from the clastic input of dunes and fluvial systems, with occasional higher energy fluvial input into the lake during humid periods (*cf.* Gierlowski-Kordesch, 1998) resulting in turbulent conditions mobilising sediment and generating Stromatactis-like cavities through settling (*cf.* Hladil, 2005,2007; Hladil *et al.,* 2006). The relative rarity of MF5 may be due to a combination of the effects of preservation potential or infrequent conditions for deposition within an arid climate. Flooding, increased clastic input, or desiccation coupled with rare periods of humidity and lower salinities results in only a limited window for carbonate generation. The occurrence of MF5 only within Log 1.7 could indicate a more central lake location, far enough away from clastic input.

The reworked appearance of MF4 is probably due to expansion of these desert lakes over the microbial mats of MF3 fed by increased fluvial discharge during climatic fluctuations, acting as a primary influence on lacustrine sedimentation within the area.

MF6

The MF6 is not a carbonate and therefore not a specific depositional microfacies. the microfacies represents the replacement of carbonate and evaporitic minerals by silica, most likely as a product of burial diagenesis (Scholle & Ulmer-Scholle, 2003). These features are typically associated with silica fabrics in chert nodules, which have replaced evaporite minerals (Milliken, 1979: Hesse, 1989). MF6 is a post-depositional process, therefore it offers little help in determining the depositional story of the formation.

Sulphate or chlorides are the most probable minerals to have been replaced, as these occur as either cements, displacive- or replacive nodules, or as interbedded strata in carbonate rocks. Whether these minerals relate directly to the precipitation and deposition of primary evaporites from concentration of saline waters, or they relate to the migration of evaporitic brines into underlying or adjacent stratigraphic units as displacive- or replacive nodules that are unrelated to evaporitic conditions, is unknown (Scholle & Ulmer-Scholle, 2003). Even after deposition and substantial burial, evaporite minerals can be remobilised and precipitated in distant and stratigraphically unrelated units (Scholle & Ulmer-Scholle, 2003).

The seemingly random distribution of the microcrystalline quartz facies (MF6) shows this facies was probably related to a selective diagenetic process, however the formation mechanism remains somewhat equivocal, though most likely attributed to the alteration of evaporitic material (Hesse, 1989). Whether specific facies are more susceptible to alteration is unclear as the primary fabrics are obliterated.

Discussion

The interpretation presented above supports a wholly continental depositional setting for the sabkha-like sediments of the Cedar Mesa Sandstone Formation. They were most likely deposited within playa-lake and lake-marginal setting along the edge of an aeolian erg, with their stratigraphical relationships probably governed principally by climatic fluctuations.

During arid times MF1 formed within isolated wet interdunes sitting in front of sinuous crested aeolian dunes. The MF3, exhibiting excellent preservation of microbial mats, formed around the edges of saline-rich playa lakes, within saline mudflats, occasional encroachment of dunes over the mats resulted in degassing, contorting and deformation of the mats, possibly exacerbated by the lateral growth of the mats into one another. Laminoid fenestrae preserved within the microbial mats indicate probable desiccation of the mats (forming cavities) followed by the subsequent colonization of said cavities by encrusting cyanobacteria.

During humid times, MF2 formed in interconnected wet interdunes formed between the crests of in-phase straight crested dunes, with frequent fluvial influx transporting and depositing clastic material. Larger perennial desert lakes flooded over previously deposited microbial mats, reworking them. Within the middle of these deeper desert lakes, MF5 formed in fresh-brackish conditions away from clastic input of the dunes and fluvial systems.

Notwithstanding this interpretation, it is worthy of note that many of the individual features of the microfacies described here are shared with heavily marine-influenced, mixed evaporite, carbonate and clastic successions, such as those of the Zechstein of Northern Europe (see Peryt et al., 2012: Tucker, 1991). These include frequent wavy microbial laminations (Steinhoff & Strohmenger, 1996), microbial crusts, and encrusting modes of formation (Peryt et al., 2012; Kiersnowski et al., 2010) indicative of shallow subaqueous to temporally sub aerial environments (Peryt et al., 2012).

However, the typically isolated and restricted spatial extent of individual facies, coupled with the spatial and temporal distribution of associated clastic sediments and the limited distribution of the sabkha-like strata, argue against a marine influence. Never-the-less, a wholly continental interpretation, as is presented here, does present two further questions.

Stanesco & Campbell (1989) present a marine influenced interpretation based upon isotopic analysis. Although this result was generated from materials susceptible to recycling of marine signatures, the likelihood of such marine recycling requires some reflection. Furthermore, if the sediments examined in this work are the deposits of a continental sabkha on the edge of an aeolian dunefield, then this rather localised area must have remained reasonable wet through time, even during periods of relative aridity in the desert system. A localised control for the wet area within the Cedar Mesa erg is required to explain the presence of the deposits.

Localised tectonics that generate tectonic lows in which water can pool and subsequently evaporate is a recognised primary control on sabkha formation (cf. Mertz & Hubert, 1989). It is possible that the arrangements of the inverted normal faults that control the Comb Ridge and Raplee Ridge monoclines (Fig. 1) may have provided this tectonic low. These faults have been dated as inherited Precambrian basement structures with multiple movement throughout geological time (Huntoon, 1993; Kelley 1955). Pre-inversion, the two antithetic extensional faults form a graben-like structure (Fig. 12) and topographic low that coincides geographically with the sabkha deposits. It may explain the location and distribution of the continental sabkha sediments, with potentially deeper facies (i.e. MF5) occurring near the point of maximum fault displacement.

In addition to channelling surface water into a topographical low, it is conceivable that the arrangements of faults may have provided further water to the sabkha low by channelling ground water to surface. If this was the case then it is conceivable that groundwater may have been in contact with the underlying marine salts of the Pennsylvanian Paradox Formation and recycling of the marine signature from the Paradox may result in the marine geochemical signature recognised by Stanesco & Campbell (1989). Significant additional analysis of geometries and structural relationships within the subsurface coupled with further in-depth isotope analyses are required to further this argument.

Conclusions

Five primary microfacies and one diagenetic ‘microfacies’ have been described for the first time within the Cedar Mesa Sandstone Formation of the Cutler Group, Utah, USA. The microfacies show evidence of preservation of ancient microbial mats and record an erg-marginal sabkha within an arid continental setting that is responding to climate variation.

The controlling factors on the location of the sabkha within a dominantly arid aeolian formation remain somewhat equivocal, but some explanation may be provided by the geometric relationships of normal faults present at the time of sediment deposition and now inverted to for the Comb and Raplee ridges.

The interpretations made here highlight the importance of a holistic sedimentary approach to the interpretation of mixed sedimentary successions that considers both the carbonate component as well as the clastic component. As such, the work complements and expands upon depositional models proposed by previous workers and provides examples of well-preserved carbonate material from a depositional environment where preservation potential (i.e. ancient microbial mats) is perhaps better than previously thought.

Acknowledgments

This research was supported by grants to RPP from the AAPG (Gustavus E. Archie Memorial Grant). The authors thank The National Park Service, the Rangers of Canyonlands National Park and the Navajo Nation for permitting field-based data collection. David Wilde, Peter Greatbatch and Adam Jeffery are thanked for thin section preparation and laboratory assistance. David Siveter is thanked for assistance in identifying ostracods. Stephen Lokier an anonymous reviewer and members of the BDRG at Keele are thanked for constructive criticism of the manuscript.

Conflict of Interest

The authors declare no conflict of interest.

Data Availability Statement

The data that support the findings of this study are available from the corresponding author upon reasonable request.

References

Ahlbrandt, T. S., & Fryberger, S. G. (1981). Sedimentary features and significance of interdune deposits. In: Recent and Ancient Nonmarine Depositional Environments: Models for Exploration (Eds F.G. Ethridge and R.M. Flores) SEPM Spec. Publ.,31, 293-314.

Aubrecht, R., Szulc, J., Michalik, J., Schlögl, J., & Wagreich, M. (2002). Middle Jurassic stromatactis mud-mound in the Pieniny Klippen Belt (Western Carpathians). *Facies*, *47*(1), 113-126. https://doi.org/10.1007/BF02667709

Bain, R. J., & Kindler, P. (1994). Irregular fenestrae in Bahamian eolianites; a rainstorm-induced origin. *Journal of Sedimentary Research*, *64*(1a), 140-146. https://doi.org/10.1306/D4267D34-2B26-11D7-8648000102C1865D

Barbeau, D. L. (2003). A flexural model for the Paradox Basin: implications for the tectonics of the Ancestral Rocky Mountains. *Basin Research*, *15*(1), 97-15.https://doi.org/10.1046/j.1365-2117.2003.00194.x

Bathurst, R. G. (1980). Stromatactis—Origin related to submarine-cemented crusts in Paleozoic mud mounds. *Geology*, *8*(3), 131-134. https://doi.org/10.1130/0091-7613(1980)8%3C131:SRTSCI%3E2.0.CO;2

Blakey, R. C. (1988). Basin tectonics and erg response. *Sedimentary Geology*, *56*(1-4), 127-151. https://doi.org/10.1016/0037-0738(88)90051-6

Blakey, R. C., Peterson, F., & Kocurek, G. (1988). Synthesis of late Paleozoic and Mesozoic eolian deposits of the Western Interior of the United States. *Sedimentary Geology*, *56*(1-4), 3-125. https://doi.org/10.1016/0037-0738(88)90050-4

Bourque, P. A., & Gignac, H. (1983). Sponge-constructed stromatactis mud mounds, Silurian of Gaspé, Québec. *Journal of Sedimentary Research*, *53*(2), 521-532. https://doi.org/10.1306/212F821F-2B24-11D7-8648000102C1865D

Chaplin, J. A., & Ayre, D. J. (1997). Genetic evidence of widespread dispersal in a parthenogenetic freshwater ostracod. *Heredity*, 78, 57-67. https://doi.org/10.1038/hdy.1997.7

Condon, S. M. (1997). Geology of the Pennsylvanian and Permian cutler group and Permian Kaibab limestone in the Paradox Basin, southeastern Utah and southwestern Colorado (No. 2000). US Government Printing Office.

Court, W. M., Paul, A., & Lokier, S. W. (2017). The preservation potential of environmentally diagnostic sedimentary structures from a coastal sabkha. *Marine Geology*, *386*, 1-18. https://doi.org/10.1016/j.margeo.2017.02.003

Davis, G. H. (1999). Structural geology of the Colorado Plateau region of southern Utah, with special emphasis on deformation bands (Vol. 342). Geological Society of America.

Delecat, S., & Reitner, J. (2005). Sponge communities from the Lower Liassic of Adnet (Northern Calcareous Alps, Austria). *Facies*, *51*(1-4), 385-404. https://doi.org/10.1007/s10347-005-0045-x

Dorney, L. J., Parrish, J. T., Chan, M. A., & Hasiotis, S. T. (2017). Petrography and Environmental Interpretation of Tufa Mounds and Carbonate Beds In the Jurassic Navajo Sandstone of Southeastern Utah, USA. Journal of Sedimentary Research, *87*(9), 967-985. https://doi.org/10.2110/jsr.2017.56

Driese, S. G. (1985). Interdune pond carbonates, Weber Sandstone (Pennsylvanian-Permian), northern Utah and Colorado. Journal of Sedimentary Research, *55*(2), 187-195. https://doi.org/10.1306/212F8661-2B24-11D7-8648000102C1865D

Dunham, R.J. (1962). Classification of carbonate rocks according to depositional texture: American Association of Petroleum Geologists, Memoir, (1), 108–121.

Flajs, G., & Hüssner, H. (1993). A microbial model for the Lower Devonian stromatactis mud mounds of the Montagne Noire (France). *Facies*, *29*(1), 179. https://doi.org/10.1007/BF02536928

Gierlowski-Kordesch, E. H. (1998). Carbonate deposition in an ephemeral siliciclastic alluvial system: Jurassic Shuttle Meadow Formation, Newark Supergroup, Hartford basin, USA. *Palaeogeography, Palaeoclimatology, Palaeoecology*, *140*(1-4), 161-184. https://doi.org/10.1016/S0031-0182(98)00039-X

Hesse, R. (1989). Silica diagenesis: origin of inorganic and replacement cherts. *Earth-Science Reviews*, *26*(1-3), 253-284. https://doi.org/10.1016/0012-8252(89)90024-X

Hilley, G. E., Mynatt, I., & Pollard, D. D. (2010). Structural geometry of Raplee Ridge monocline and thrust fault imaged using inverse Boundary Element Modeling and ALSM data. *Journal of Structural Geology*, *32*(1), 45-58. https://doi.org/10.1016/j.jsg.2009.06.015

Hintze, L.F. (1980). Geological Map of Utah, *Utah Geological & Mineral Survey*, Map A-1, 1:500,000

Hladil J.I, Koptikova L, Ruzicka M, Kulaviak LU. (2007). Experimental effects of surfactants on the production of stromatactis-shaped cavities in artificial carbonate sediments. *Bulletin of Geosciences*, *82*(1), 37-50.

Hladil J.I, Růžička M, Koptíková LE. (2006). Stromatactis cavities in sediments and the role of coarse-grained accessories. *Bulletin of Geosciences*, *81*(2), 123-146.

Hladil, J.I. (2005). The formation of stromatactis-type fenestral structures during the sedimentation of experimental slurries—a possible clue to a 120-year-old puzzle about stromatactis. *Bulletin of Geosciences*, *80*(3), 193-211.

Howell, J. and Mountney, N. (1997) Climatic cyclicity and accommodation space in arid to semi-arid depositional systems: an example from the Rotliegend Group of the UK southern North Sea. In: Petroleum Geology of the Southern North Sea: Future Potential (Eds K. Ziegler, P. Turner and S.R. Daines), Geol. Soc. London Spec. Publ., 123, 63–86. https://doi.org/10.1144/GSL.SP.1997.123.01.05

Huntoon, J. E., Stanesco, J. D., Dubiel, R. F., & Dougan, J. (2000). Geology of Natural Bridges National Monument, Utah. *Geology of Utah's Parks and Monuments: Utah Geological Association, Publication*, *28*, 233-249.

Huntoon, P. W. (1993). Influence of inherited Precambrian basement structure on the localization and form of Laramide monoclines, Grand Canyon, Arizona. *Geological Society of America Special Papers*, *280*, 243-256.

Jordan, O. D., & Mountney, N. P. (2010). Styles of interaction between aeolian, fluvial and shallow marine environments in the Pennsylvanian to Permian lower Cutler beds, south-east Utah, USA. *Sedimentology*, *57*(5), 1357-1385. https://doi.org/10.1111/j.1365-3091.2010.01148.x

Jordan, O. D., & Mountney, N. P. (2012). Sequence stratigraphic evolution and cyclicity of an ancient coastal desert system: the Pennsylvanian–Permian Lower Cutler Beds, Paradox Basin, Utah, USA. *Journal of Sedimentary Research*, *82*(10), 755-780.https://doi.org/10.2110/jsr.2012.54

Kelley, V. C. (1955). Monoclines of the Colorado Plateau. *Geological Society of America Bulletin*, *66*(7), 789-804. https://doi.org/10.1130/0016-7606(1955)66[789:MOTCP]2.0.CO;2

Kiersnowski, H., Peryt, T. M., Buniak, A., & Mikołajewski, Z. (2010). From the intra-desert ridges to the marine carbonate island chain: middle to late Permian (Upper Rotliegend–Lower Zechstein) of the Wolsztyn–Pogorzela high, west Poland. *Geological Journal*, *45*(2-3), 319-335.

Kocurek, G. (1981). Significance of interdune deposits and bounding surfaces in aeolian dune sands. *Sedimentology*, *28*(6), 753-780. https://doi.org/10.1111/j.1365-3091.1981.tb01941.x

Kukal, Z. (1971). Open-space structures in the Devonian limestones of the Barrandian (Central Bohemia). *Cas Mineral Geol*, *16*, 345-362.

Langford, R. P., & Chan, M. A. (1989). Fluvial-aeolian interactions: Part II, ancient systems. *Sedimentology*, *36*(6), 1037-1051. https://doi.org/10.1111/j.1365-3091.1989.tb01541.x

Langford, R., & Chan, M. A. (1988). Flood surfaces and deflation surfaces within the Cutler Formation and Cedar Mesa Sandstone (Permian), southeastern Utah. *Geological Society of America Bulletin*, *100*(10), 1541-1549. https://doi.org/10.1130/0016-7606(1988)100%3C1541:FSADSW%3E2.3.CO;2

Langford, R.P. and Massad, A. (2014) Facies geometries and climatic influence on stratigraphy in the eolian-sabkha transition in the Permian Cedar Mesa Sandstone, SE Utah In: Geology of Utah’s Far South, (Eds J.S.MacLean, R.F. Biek, and J.E. Huntoon) Utah Geological Association Publication, 43, 275-294.

Lokier, S. W., & Al Junaibi, M. (2016). The petrographic description of carbonate facies: are we all speaking the same language?. *Sedimentology*, *63*(7), 1843-1885. https://doi.org/10.1111/sed.12293

Lokier, S. W., Andrade, L. L., Court, W. M., Dutton, K. E., Head, I. M., van der Land, C., ... & Sherry, A. (2017). A new model for the formation of microbial polygons in a coastal sabkha setting. *The Depositional Record*, *3*(2), 201-208. https://doi.org/10.1002/dep2.33

Loope, D. B. (1984). Eolian origin of upper Paleozoic sandstones, southeastern Utah. *Journal of Sedimentary Research*, *54*(2), 563-580. https://doi.org/10.1306/212F846D-2B24-11D7-8648000102C1865D

Lowenstein, T. K., & Hardie, L. A. (1985). Criteria for the recognition of salt-pan evaporites. *Sedimentology*, *32*(5), 627-644. https://doi.org/10.1111/j.1365-3091.1985.tb00478.x

May, G., Hartley, A. J., Stuart, F. M., & Chong, G. (1999). Tectonic signatures in arid continental basins: an example from the Upper Miocene–Pleistocene, Calama Basin, Andean forearc, northern Chile. *Palaeogeography, Palaeoclimatology, Palaeoecology*, *151*(1-3), 55-77. https://doi.org/10.1016/S0031-0182(99)00016-4

McKay, C. P., Rask, J. C., Detweiler, A. M., Bebout, B. M., Everroad, R. C., Lee, J. Z., ... & Al-Awar, M. (2016). An unusual inverted saline microbial mat community in an interdune sabkha in the Rub'al Khali (the Empty Quarter), United Arab Emirates. *PloS one*, *11*(3), e0150342. https://doi.org/10.1371/journal.pone.0150342

Mertz Jr, K. A., & Hubert, J. F. (1990). Cycles of sand-flat sandstone and playa–lacustrine mudstone in the Triassic–Jurassic Blomidon redbeds, Fundy rift basin, Nova Scotia: implications for tectonic and climatic controls. *Canadian Journal of Earth Sciences*, *27*(3), 442-451.https://doi.org/10.1139/e90-039

Mettraux, M., Homewood, P. W., Kwarteng, A. Y., & Mattner, J. (2011). Coastal and continental sabkhas of Barr Al Hikman, Sultanate of Oman. *International Association of Sedimentology Spec. Publ*, *43*, 183-204.

Milliken, K. L. (1979). The silicified evaporite syndrome; two aspects of silicification history of former evaporite nodules from southern Kentucky and northern Tennessee. *Journal of Sedimentary Research*, *49*(1), 245-256. https://doi.org/10.1306/212F7707-2B24-11D7-8648000102C1865D

Monty, C. L. (1995). The rise and nature of carbonate mud-mounds: an introductory actualistic approach. *Carbonate Mud-Mounds: Their Origin and Evolution*, 11-48. https://doi.org/10.1002/9781444304114.ch2

Mountney, N. P. (2006). Periodic accumulation and destruction of aeolian erg sequences in the Permian Cedar Mesa Sandstone, White Canyon, southern Utah, USA. *Sedimentology*, *53*(4), 789-823. https://doi.org/10.1111/j.1365-3091.2006.00793.x

Mountney, N. P. (2012). A stratigraphic model to account for complexity in aeolian dune and interdune successions. *Sedimentology*, *59*(3), 964-989. https://doi.org/10.1111/j.1365-3091.2011.01287.x

Mountney, N. P., & Jagger, A. (2004). Stratigraphic evolution of an aeolian erg margin system: the Permian Cedar Mesa Sandstone, SE Utah, USA. *Sedimentology*, *51*(4), 713-743. https://doi.org/10.1111/j.1365-3091.2004.00646.x

Müller-Jungbluth, W. U., & Toschek, P. H. (1969). *Karbonatsedimentologische Arbeitsgrundlagen: Begriffe, Erläuterungen, Hinweise* (No. 4). In Kommissionsverlag der Österreichischen Kommissionsbuchhandlung.

Mynatt, I., Seyum, S., & Pollard, D. D. (2009). Fracture initiation, development, and reactivation in folded sedimentary rocks at Raplee Ridge, UT. *Journal of Structural Geology*, *31*(10), 1100-1113. https://doi.org/10.1016/j.jsg.2009.06.003

Parrish, J. T., Hasiotis, S. T., & Chan, M. A. (2017). Carbonate Deposits In the Lower Jurassic Navajo Sandstone, Southern Utah and Northern Arizona, USA. *Journal of Sedimentary Research*, *87*(7), 740-762. https://doi.org/10.2110/jsr.2017.42

Peryt, T. M., Raczyński, P., Peryt, D., & Chłódek, K. (2012). Upper Permian reef complex in the basinal facies of the Zechstein Limestone (Ca1), western Poland. *Geological Journal*, *47*(5), 537-552. https://doi.org/10.1002/gj.2440

Platt, N. H. (1989). Lacustrine carbonates and pedogenesis: sedimentology and origin of palustrine deposits from the Early Cretaceous Rupelo Formation, W Cameros Basin, N Spain. Sedimentology, *36*(4), 665-684. https://doi.org/10.1111/j.1365-3091.1989.tb02092.x

Riding, R. (2000). Microbial carbonates: the geological record of calcified bacterial–algal mats and biofilms. *Sedimentology*, *47*, 179-214. https://doi.org/10.1046/j.1365-3091.2000.00003.x

Rogers, S. L. (2018). A novel population of composite mounds: their initiation, growth and demise. San Emiliano Formation, Cantabrian Mountains, Spain. *Journal of Iberian Geology*, 1-17. https://doi.org/10.1007/s41513-018-0056-4

Rubin, D. M. (1987). Formation of scalloped cross-bedding without unsteady flows. *Journal of Sedimentary Research*, *57*(1), 39-45. https://doi.org/10.1306/212F8A99-2B24-11D7-8648000102C1865D

Rubin, D.M. and Carter, C.L. (2006) Cross-bedding, bedforms, and paleocurrents. SEPM Concepts Sedimentol. Paleontol., 1, 2nd edn, 195 p.

Sanz, M. E., Zarza, A. A., & Calvo, J. P. (1995). Carbonate pond deposits related to semi-arid alluvial systems: examples from the Tertiary Madrid Basin, Spain. Sedimentology, 42(3), 437-452. https://doi.org/10.1111/j.1365-3091.1995.tb00383.x

Scholle, P. A., & Ulmer-Scholle, D. S. (2003). A Color Guide to the Petrography of Carbonate Rocks: Grains, Textures, Porosity, Diagenesis, AAPG Memoir 77 (Vol. 77). AAPG.

Seard, C., Camoin, G., Rouchy, J. M., & Virgone, A. (2013). Composition, structure and evolution of a lacustrine carbonate margin dominated by microbialites: Case study from the Green River formation (Eocene; Wyoming, USA). Palaeogeography, Palaeoclimatology, Palaeoecology, *381*, 128-144. https://doi.org/10.1016/j.palaeo.2013.04.023

Shinn, E. A. (1968). Practical significance of birdseye structures in carbonate rocks. *Journal of Sedimentary Research*, *38*(1), 215-223. https://doi.org/10.1306/74D7191F-2B21-11D7-8648000102C1865D

Spötl, C., & Wright, V. P. (1992). Groundwater dolocretes from the Upper Triassic of the Paris Basin, France: a case study of an arid, continental diagenetic facies. Sedimentology, *39*(6), 1119-1136. https://doi.org/10.1111/j.1365-3091.1992.tb02000.x

Stanesco, J. D., & Campbell, J. A. (1989). Eolian and noneolian facies of the lower Permian Cedar Mesa Sandstone Member of the Cutler Formation, southeastern Utah. *US Geol. survey bull.; 1808, Chap. F. Evolution of sedimentary basins-San Juan basin*.

Steinhoff, I., & Strohmenger, C. (1996). Zechstein 2 carbonate platform subfacies and grain-type distribution (Upper Permian, northwest Germany). *Facies*, 35(1), 105-132. https://doi.org/10.1007/BF02536959

Stenzel, S. R., & James, N. P. (1995). Shallow-Water Stromatactis Mud-Mounds on a Middle Ordovician Foreland Basin Platform, Western Newfoundland. *Carbonate Mud-Mounds: Their Origin and Evolution*, 125-149. https://doi.org/10.1002/9781444304114.ch4

Taberner, C., Cendón, D. I., Pueyo, J. J., & Ayora, C. (2000). The use of environmental markers to distinguish marine vs. continental deposition and to quantify the significance of recycling in evaporite basins. *Sedimentary Geology*, *137*(3-4), 213-240. https://doi.org/10.1016/S0037-0738(00)00105-6

Tanner, L. H., & Lucas, S. G. (2010). Deposition and deformation of fluvial–lacustrine sediments of the Upper Triassic–Lower Jurassic Whitmore Point Member, Moenave Formation, northern Arizona. *Sedimentary Geology*, *223*(1-2), 180-191. https://doi.org/10.1016/j.sedgeo.2009.11.010

Tebbutt, G. E., Conley, C. D., & Boyd, D. W. (1965). Lithogenesis of a distinctive carbonate rock fabric. *Rocky Mountain Geology*, *4*(1), 1-13.

Tsien, H. H. (1985). Origin of stromatactis—a replacement of colonial microbial accretions. In *Paleoalgology* (pp. 274-289). Springer, Berlin, Heidelberg.

Tucker, M. E. (1991). Sequence stratigraphy of carbonate-evaporite basins: models and application to the Upper Permian (Zechstein) of northeast England and adjoining North Sea. *Journal of the Geological Society*, 148(6), 1019-1036. https://doi.org/10.1144/gsjgs.148.6.1019

Van Gemerden, H. (1993). Microbial mats: a joint venture. *Marine Geology*, *113*(1-2), 3-25. https://doi.org/10.1016/0025-3227(93)90146-M

Wallace, M. W. (1987). The role of internal erosion and sedimentation in the formation of stromatactis mudstones and associated lithologies. *Journal of Sedimentary Research*, *57*(4), 695-700. https://doi.org/10.1306/212F8BDE-2B24-11D7-8648000102C1865D

Warke, M. R., Edwards, N. P., Wogelius, R. A., Manning, P. L., Bergmann, U., Egerton, V. M., ... & Schröder, S. (2019). Decimeter-scale mapping of carbonate-controlled trace element distribution in Neoarchean cuspate stromatolites. *Geochimica et Cosmochimica Acta*. *261*, 56-75. https://doi.org/10.1016/j.gca.2019.07.004

Warren, J. K. (1983). Tepees, modern (southern Australia) and ancient (Permian—Texas and New Mexico)—a comparison. *Sedimentary Geology*, *34*(1), 1-19. https://doi.org/10.1016/0037-0738(83)90032-5

Figure Captions

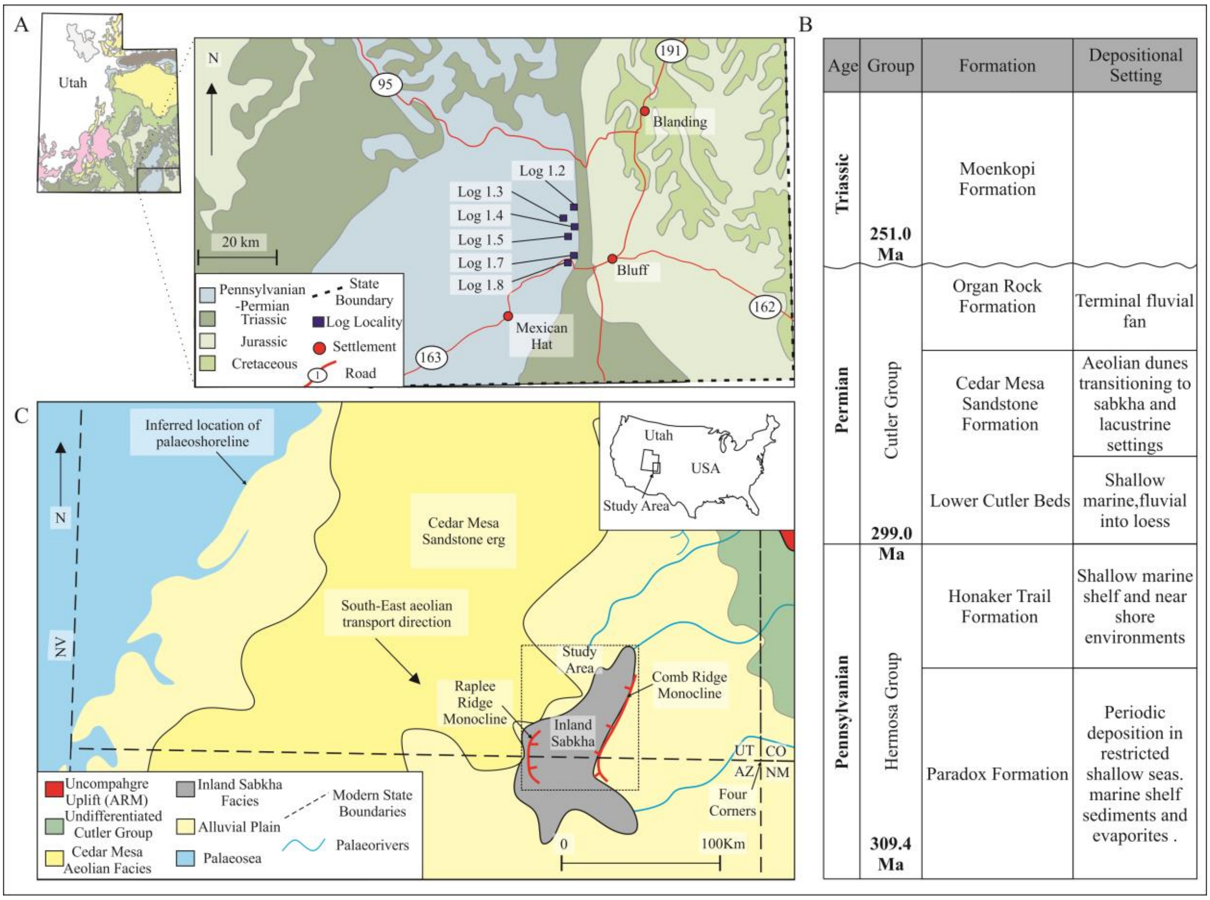

Figure 1 (A) Simplified 1:500,000 scale geological map of Utah (modified after Hintze, 1980) Log localities are superimposed and highlighted by blue boxes. State outline of Utah is indicated by dashed lines, roads are marked by solid red lines, whilst modern settlements are indicated with a red circle. **(B)** Stratigraphic setting and depositional setting of the study area from Pennsylvanian to Triassic. Unconformities are marked with an undulating line (after Barbeau, 2003). **(C)** Palaeogeographic reconstruction of the early Permian Cedar Mesa Sandstone Formation (after Blakey 1988). The aeolian dune field location is shown in dark yellow, the sabkha facies are shown in dark grey. Red indicates location of faults, ticks indicate the downthrown side. Modern state outlines are superimposed, shown by dashed line.

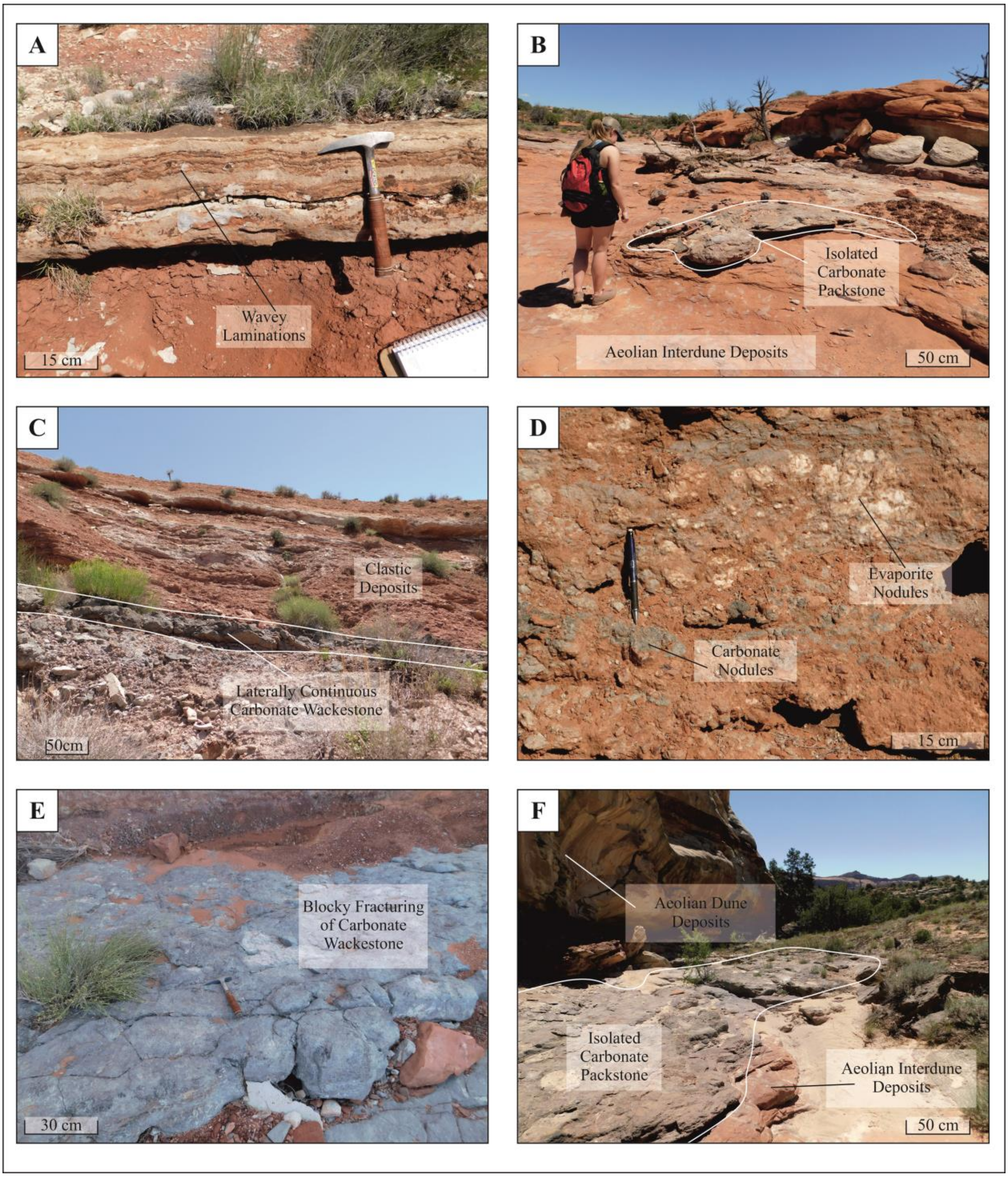

Figure 2 Outcrop photos showing the variety in carbonate deposits at field scale. **(A)** Alternating wavy laminations of carbonate wackestone, beds are laterally persistent and average approximately 40 cm thick. **(B)** Isolated lenses of clastic-rich carbonate wackestone (circled) interbedded within aeolian interdune deposits. **(C)** Thin, laterally continuous dark grey carbonate wackestone, interbedded within lacustrine clastic deposits. **(D)** Interbedded gypsum evaporite nodules (white) and carbonate nodules (grey) within a fine grained clastic matrix. **(E)** Blue carbonate wackestone, with distinctive blocky-

style fracturing. **(F)** Isolated carbonate packstone (circled) interbedded between aeolian dune and interdune deposits.

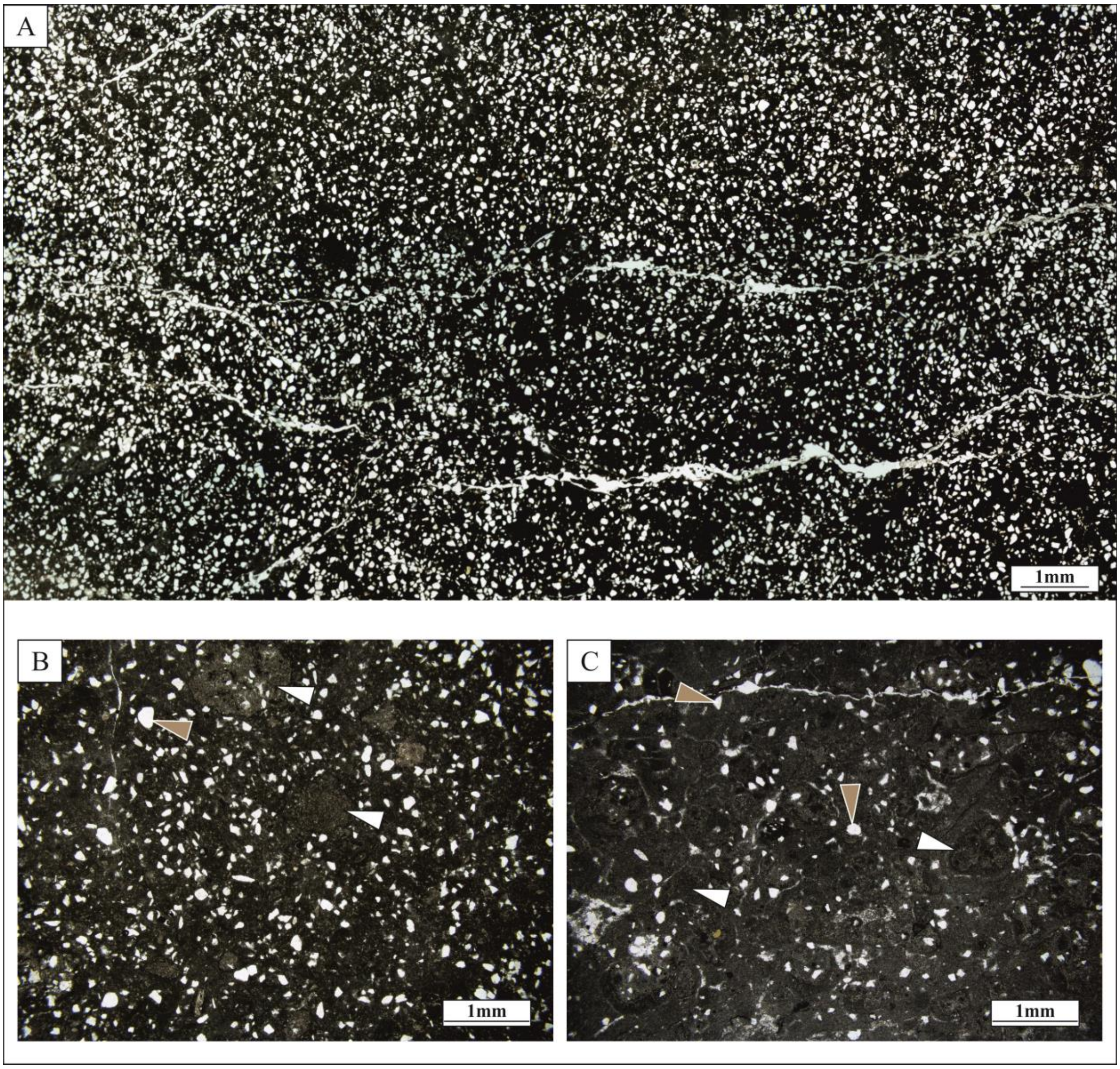

Figure 3 (A) Photomicrograph of MF1 showing the high quartz content and poorly defined laminations. **(B)** Close up of MF1 showing the dark brown carbonate mud matrix and occasional mudstone grains (white arrow) supporting clastic quartz grains (brown arrow). Clastic grains form up to 50–60% of the sample and are well sorted, with a sub-rounded to rounded texture. **(C)** Increased matrix/clast ratio and mudstone grains with microspar components (white arrow), quartz grains also highlighted (brown arrow). The mudstone grains appear to have micritic envelopes and occasional protostromate features are discernible.

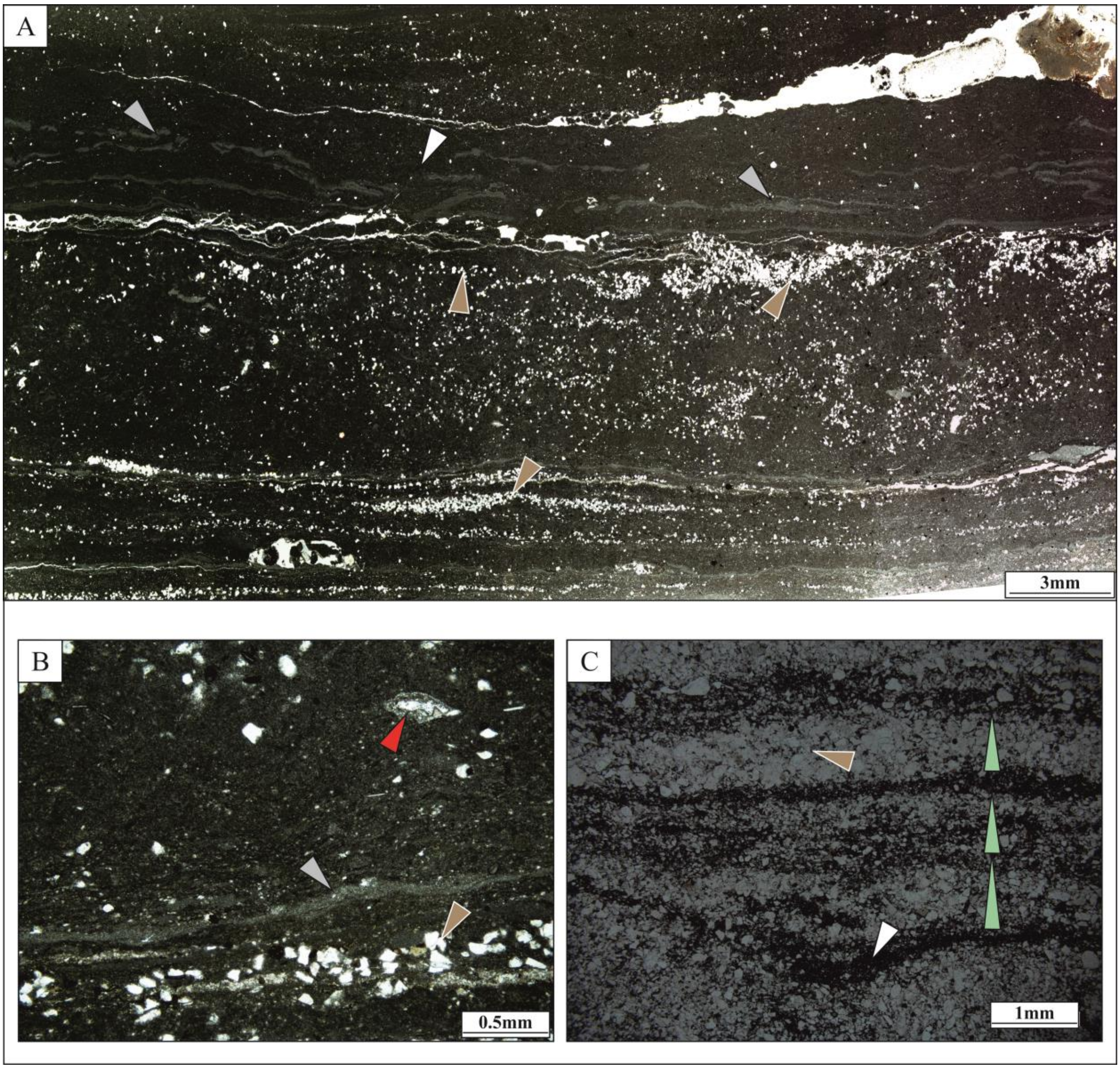

Figure 4 (A) Representative photomicrograph of MF2, the microfacies is characterised by horizontally laminated dark brown carbonate mudstone matrix (white arrow) alternating with laminated quartz grains (brown arrow) with occasional slight undulose laminations of light brown to grey microbial clotted fabrics (grey arrow). Quartz grains are reasonably well sorted and show a rounded to sub rounded texture. **(B)** The sample shows one example of an Podocopa ostracod oriented with laminations (red arrow), but otherwise is barren of skeletal grains. Brown arrow shows sub rounded quartz grains, microbial laminations are also present (grey arrow). **(C)**This sample is dominated by bedding parallel laminations of quartz grains (brown arrow), these alternate with thin flat-to-undulose brown carbonate mud matrix (white arrow). The quartz grains are moderately sorted and show a well-rounded to sub-rounded texture. The quartz laminations show a slight normal grading

with the thicker quartz bands being composed of coarser grains which normally grade upwards to finer material (green arrows point in the direction of fining).

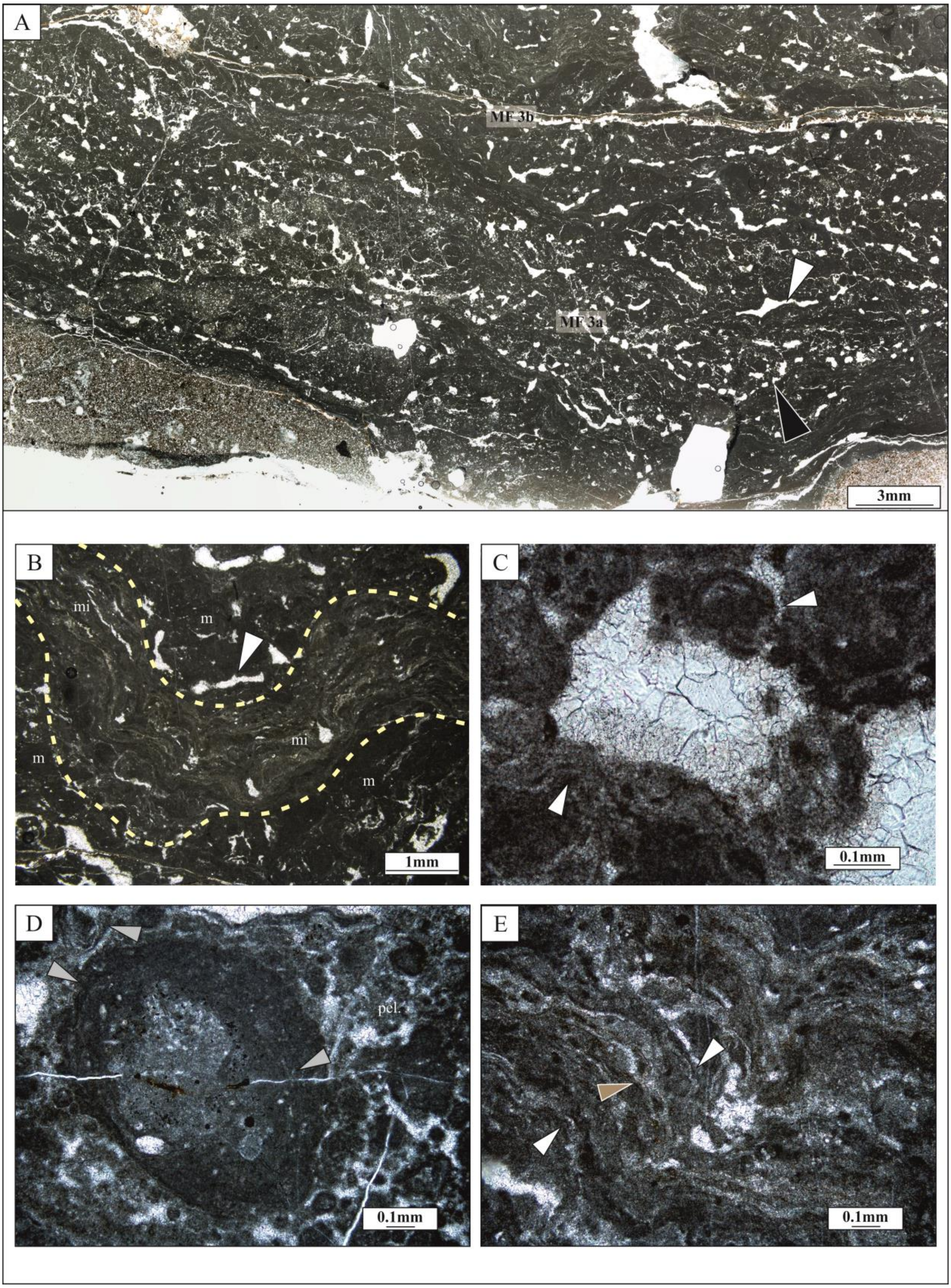

Figure 5. Photomicrographs of MF3. **(A)** image showing the multiple alternating undulose microbial bands and the change between the peloid and oncoid dominated MF3a in the middle of the figure and highly laminated MF3b. An example of an elongate fenestrae (typical of MF3a) is highlighted with a white arrow, an example of a chain-like fenestrae (also typical of MF3a) is highlighted with a black arrow. **(B)** MF3b is highlighted (outlined by dashed lines and highlighted by 'mi'.) The sub-microfacies exhibits an undulose habit and lacks the elongate fenestrae observed in MF3a. The homogenous matrix of MF3a is highlighted by 'm' an elongate fenestrae (typical of MF3a) is highlighted with a white arrow. **(C)** A typical cavity showing late blocky calcite cement fill, with a possible fibrous isopachous rim. The cavity is framed by protostromate structures. The white arrows highlight tube like structures reminiscent of *Girvanella.* **(D)** A typical oncoid found within MF3, the clast is surrounded by a matrix of peloids (pel.) which often show a clotted or thrombolytic texture. The cortex of the oncoid, and several of the peloids exhibit well preserved protostromate features (arrows), these are mostly tube like and as with the previous examples, resemble *Girvanella*. **(E)** Undulous laminations of MF3b, the white arrows highlight tube like structures whilst the middle (brown) arrow highlights an encrusting form consisting of a chain of sausage or bean-shaped chambers, this encruster is reminiscent of the calci-microbe *Rothpletzella*.

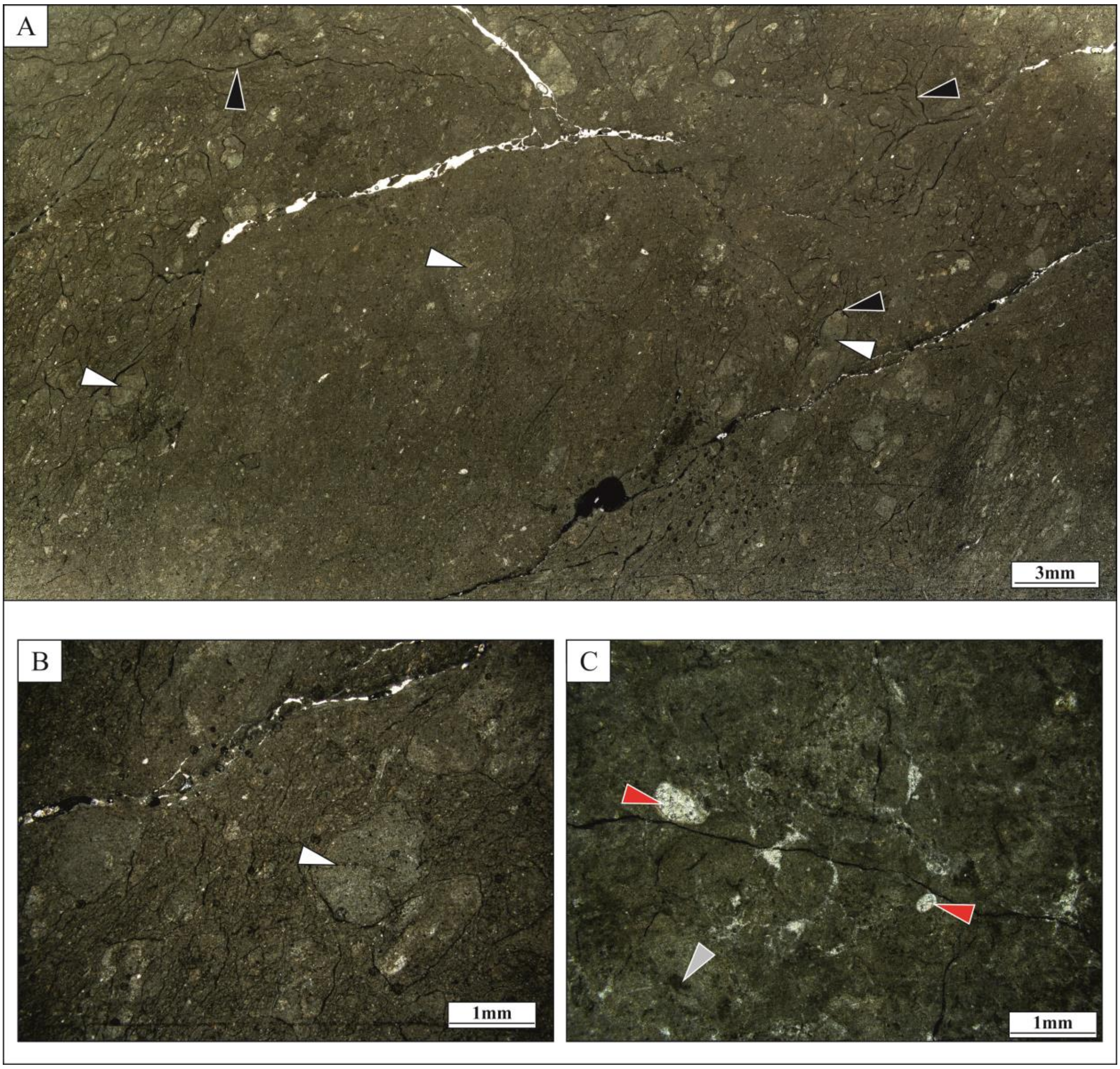

Figure 6 (A) Photomicrograph of MF 4. This sample is characterised by a dominant background matrix of massive dark brown carbonate mud with a few mud grains, often lighter in colour (white arrow). Compressional fractures (stylolites) are also present (black arrow). **(B)** This sample shows the dominant dark brown carbonate mud matrix with few mud grains (arrowed). (**C)** This sample shows a homogenous matrix of brown carbonate mud with minimal skeletal Podocopa ostracod grains (red arrow) between 30–70µm. Isolated clotted microbial textures are also present (grey arrow).

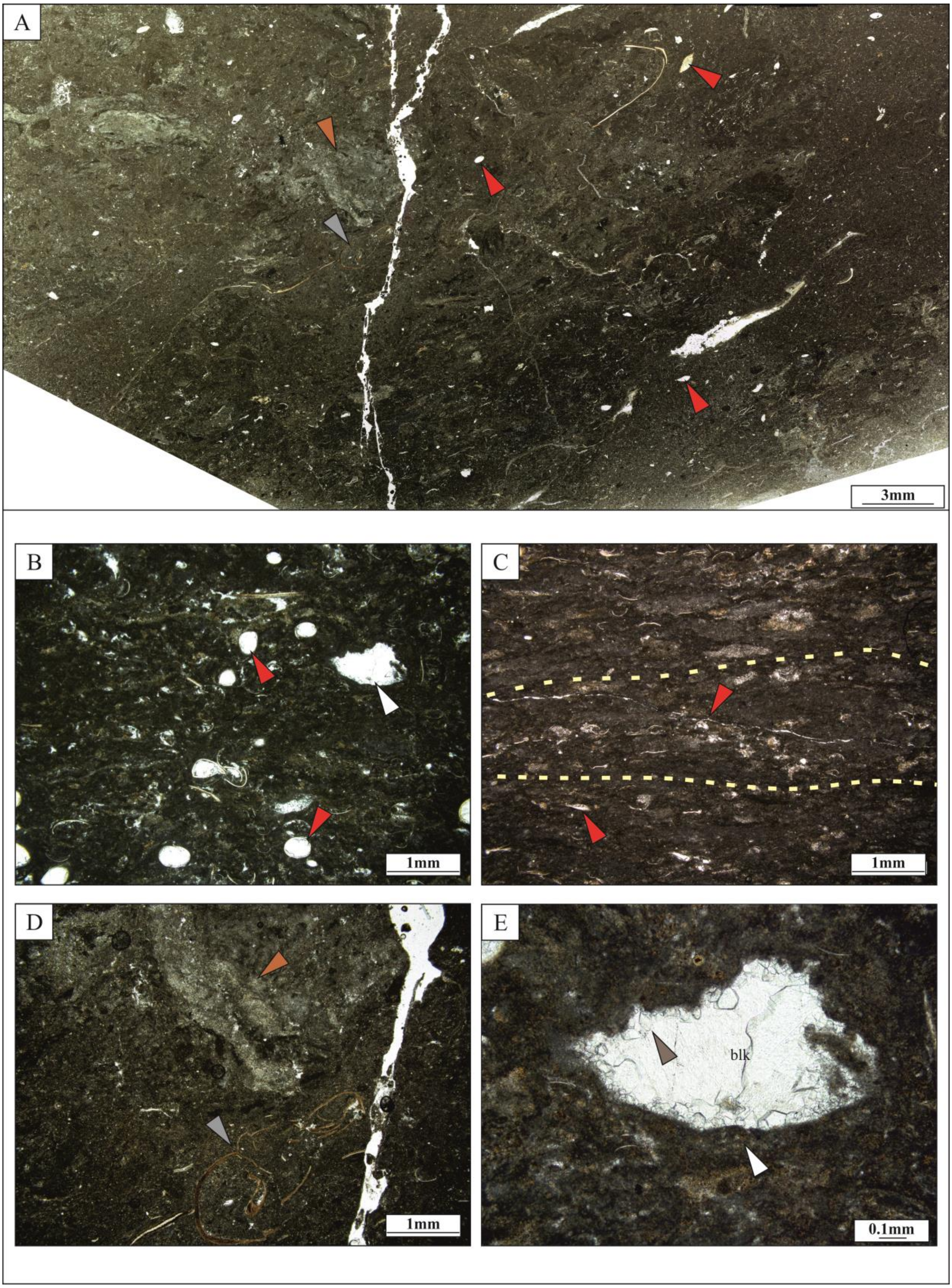

Figure 7 (A) Photomicrograph of MF5 showing the abundance of ostracods (red arrow) and occasional shell fragments (grey arrow), light clasts are shown by the orange arrow. **(B)** This sample contains abundant cross-sections through carapaces and individual valves of Podocopa ostracods (red

arrow) and potential stomatactis-like cavities (white arrow) (see Fig7 E). **(C)** The crudely laminated carbonate mud matrix interspersed with clasts of a lighter grey/green carbonate mud. Red arrow shows several complete ostracods (30–70µm) arranged in a bedding parallel fashion, the broken skeletal grains show a dominant convex upwards arrangement along a horizontal plane (yellow). **(D)** Th**e** lighter clasts highlighted in **(C)** are shown in more detail here (orange arrow). These clasts show evidence of laminations and of a clotted (sometimes thrombolytic) texture, the example highlighted here is reminiscent of the undulous microbially dominated fabric observed in MF3b. Shell fragment is highlighted by grey arrow. **(E)** A stromatactis-like cavity, the flat base and undulous roof is apparent, as is the sediment fill at the base of the cavity (red arrow). Late blocky calcite cement fills the cavities interior, (blk.) whilst a rim of smaller calcite cement lines the cavity. It is this rimming cement that distinguishes these cavities from 'true' stromatactis, voids with bare isopachous, fibrous rims.

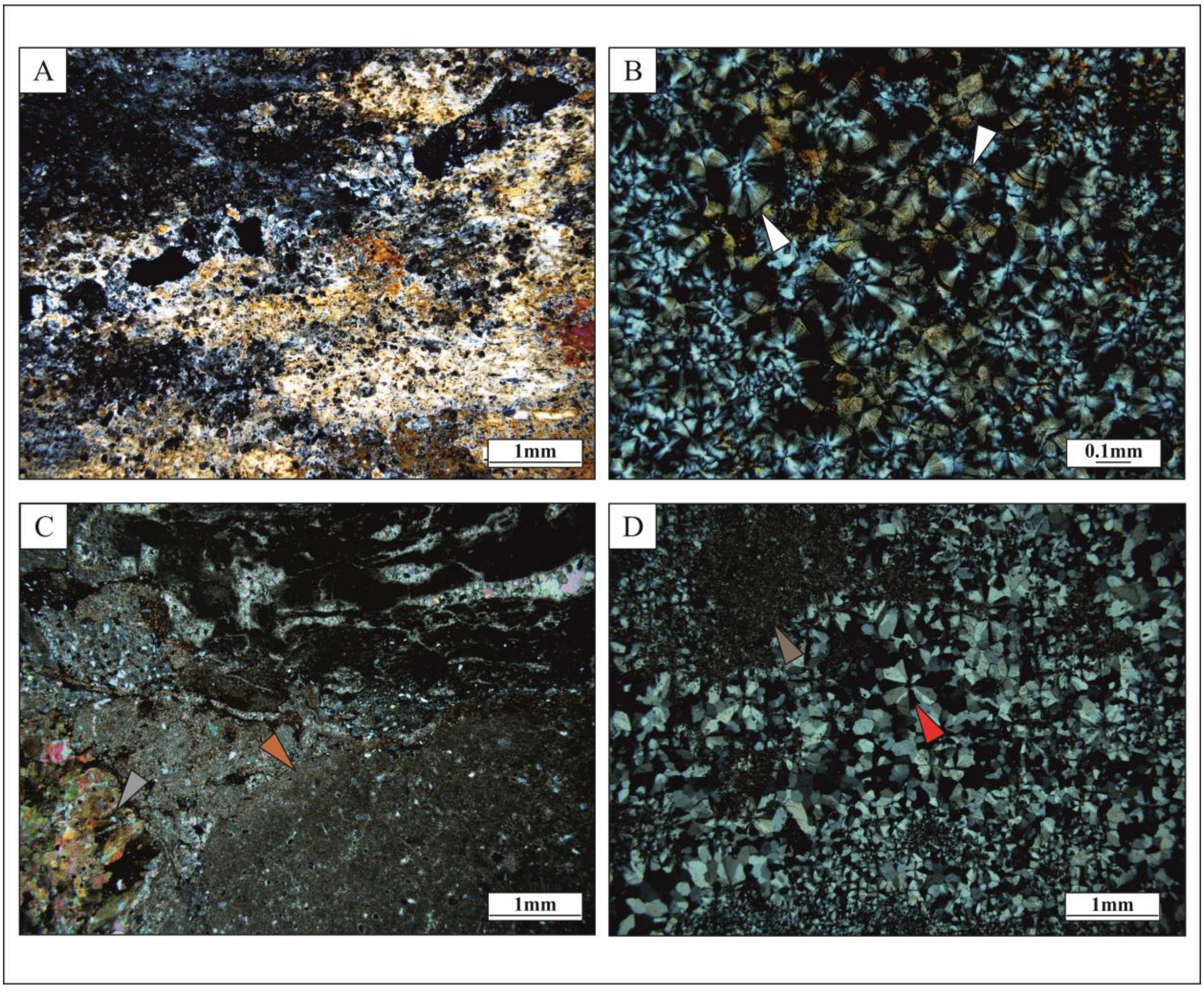

Figure 8 Photomicrograph of MF6. **(A)** High interference colours and fibrous nature under xpl. **(B)** Rimmed and radial nature of quartz crystals (arrowed). **(C)** Evaporitic inclusions (brown arrow) and displacement of original carbonate material (orange arrow), filled fractures of fibrous microquartz also present (arrow). **(D)** Radial megaquartz (red arrow) displaced primary carbonate (brown arrow)

Code	**Lithology & Texture**	**Sedimentary Structures**	**Interpretation**	**Related Associations**
Stxb	Grey to orange, fine- to medium-grained quartz arenite, well sorted & well rounded.	Trough cross-bedding with mm/cm scale alternations in grainsize in single or multiple sets.	Migration of wind-blown sinuous-crested dune-scale bedforms and dune trains.	Aeolian Dune
Sxb	Grey to orange, fine- to medium-grained quartz arenite, well sorted & well rounded	Planar cross-bedding with mm/cm scale alternations in grainsize in single or multiple sets, localised soft sediment deformation.	Migration of wind-blown straight-crested dune-scale bedforms and dune trains. Soft sediment deformation formed as a result of loading on a damp substrate.	Aeolian Dune
Sm	Grey to orange, fine- to medium-grained quartz arenite, well sorted & well rounded.	Structureless, localised desiccation cracks and root traces.	Suspension settling of wind-blown sediment in areas affected by surface water, followed by drying.	Aeolian Interdune

Sfo	Dark brown siltstone, sporadic mottling.	Parallel to faint undulose laminations, localised rhizoliths, desiccation cracks and bioturbation.	Suspension fall out from stationary waters. Stabilisation for vegetation to develop	Aeolian Interdune, Fluvial Sheetflood, Lacustrine
Sfxb	Brown medium-grained sub-arkosic arenite to quartz arenite, moderately sorted & sub-rounded.	Planar cross-bedding with normal grading, in single or multiple sets, sporadic mud clasts.	Migration of straight-crested dune-scale bedforms and dune trains sub aqueously under lower flow regime conditions.	Fluvial Sheetflood, Lacustrine
Swr	Dark brown siltstone-to fine-grained sub-arkosic arenite, moderately sorted & sub-rounded	Parallel laminations with a sporadic undulose texture and symmetrical wave ripple cross lamination.	Low energy, sub-aqueous setting, where the deposits have settled out of suspension. Undulose and wave ripples form due to oscillating waters in response to wind action within shallow waters.	Aeolian Interdune, Fluvial Sheetflood, Lacustrine
Ssl	Dark brown- to black, siltstone-to very fine-grained sandstone, sporadic mottling	Massive to faint parallel laminations with normal grading and fines upwards, high organic content.	Suspension fall out within low energy waters. High organic content indicates either thermal stratification or anoxic conditions.	Lacustrine
G	White- to peach crystalline gypsum	Massive or laminated bands of enterolithic convoluted folds or polygonal hummocks.	Precipitation from shallow saline waters and displacive growth of evaporites within saline saturated sediment.	Saline Pan, Aeolian Interdune
Gspl	Pastel blue, very fine- to fine-grained, moderate to poorly sorted, sub-rounded sub-arkosic arenite with a gypsiferous matrix and cement.	Parallel-laminated to massive, often contorted by small gypsum nodules.	Flow of saline fluid and subsequent precipitation of gypsum in the pore space of sediment around the margins of saline lakes as water evaporated at the ground surface.	Saline Pan

Table 1 Summary table detailing the sedimentary facies present in the Cedar Mesa Sandstone Formation. Each facies is given a code and described in terms of its lithology and texture and sedimentary structures present. Interpretation is based on depositional process and linked to related sedimentary associations

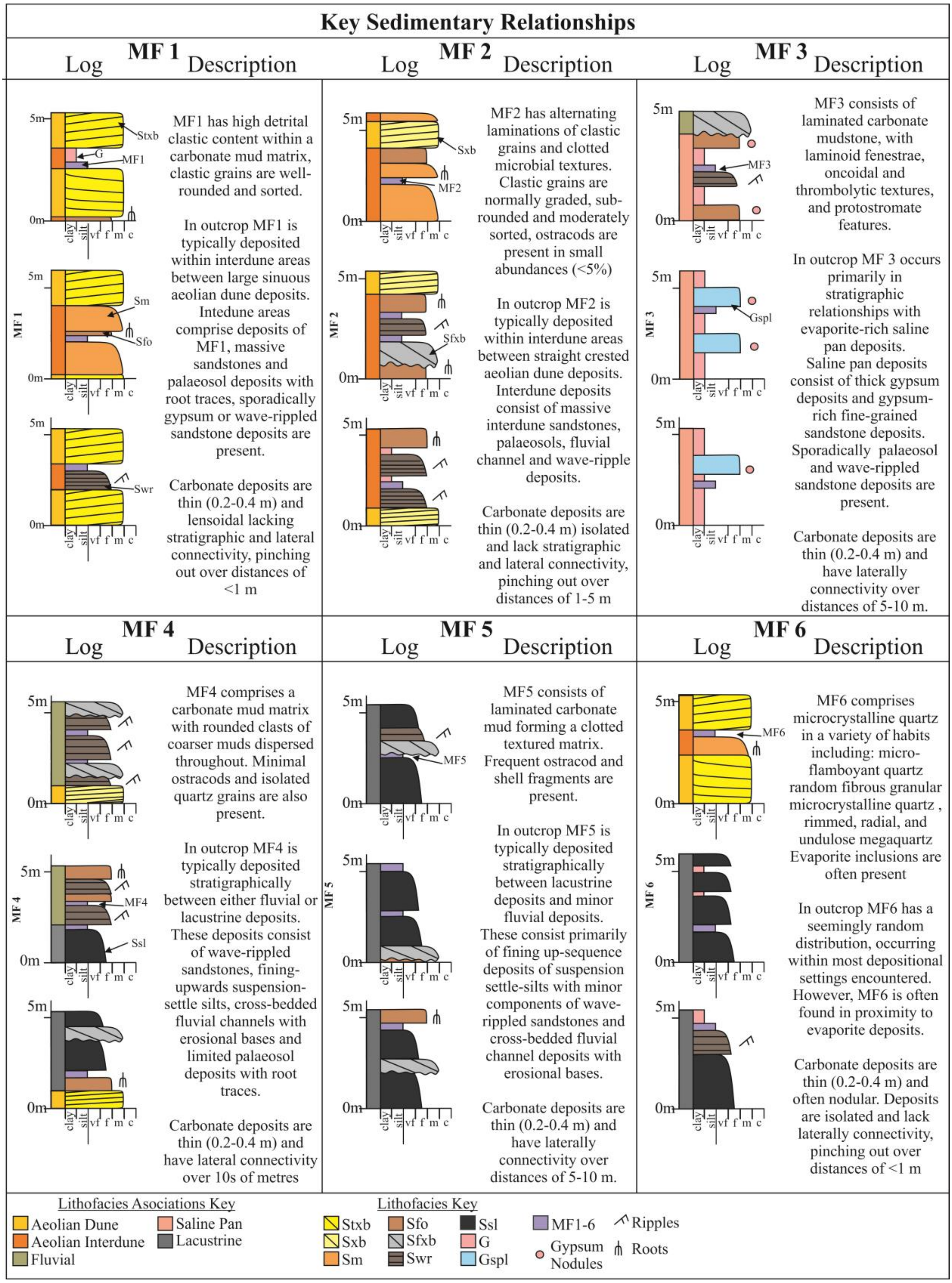

Figure 9 Key sedimentary relationships for each microfacies. Typical field relationships between each carbonate microfacies and coeval clastic/evaporitic deposits are shown within the logs. Full information about clastic facies can be found in table 1.

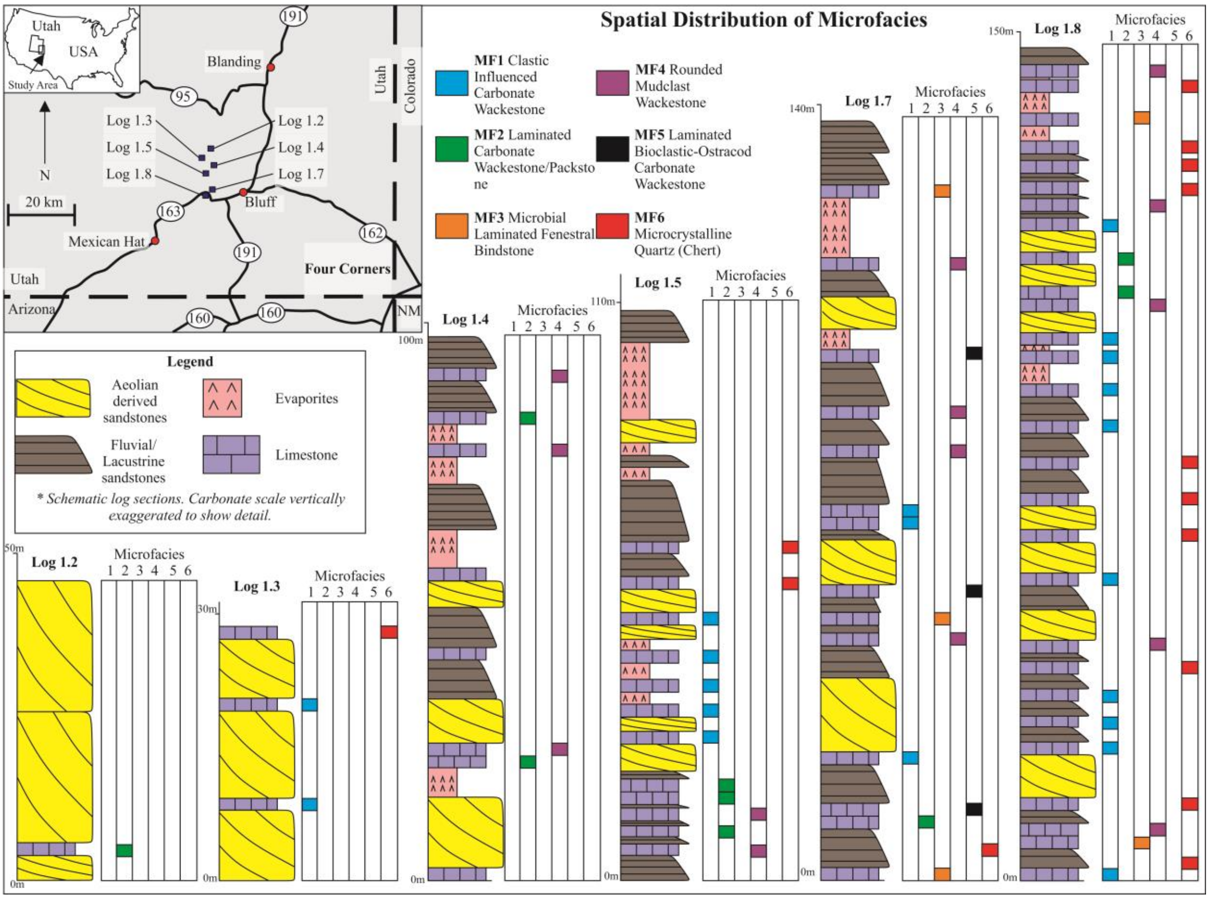

Figure 10 Schematic logs showing the spatial distribution of microfacies within the context of coeval clastic deposits. Insert in top left shows a location map, with individual log localities highlighted by blue squares, state boundaries are shown by dashed line, major roads are shown with solid black line. Logs are arranged in a north-south transect, from left to right. Logs are schematic and simplified, clastic and evaporitic bed thicknesses are true whereas carbonate beds have been exaggerated to highlight their spatial distribution. Corresponding microfacies related to the carbonate beds are shown to the right of each schematic log. Colours represent individual microfacies, explained in the key at the top of the figure. The type of deposit is explained in the legend.

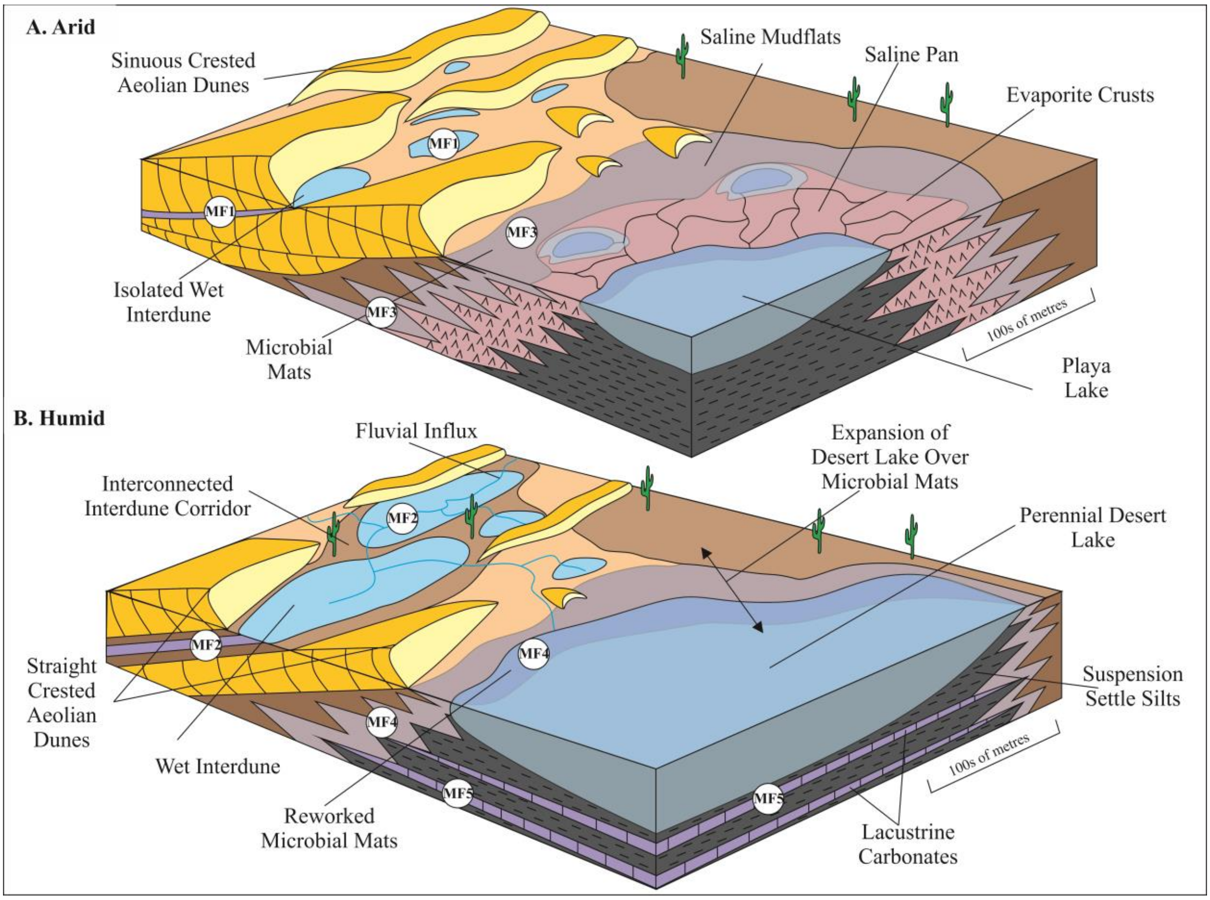

Figure 11 Depositional models for arid or humid climates which show the interpreted depositional environment for each microfacies and relationships with coeval clastic environments. Arid conditions are shown in model A, humid conditions in model B. The location of each microfacies are marked with white circles, with the number representing the corresponding microfacies. Model A shows arid times and large sinuous aeolian dunes, with small isolated wet interdunes shown in blue. Sabkha deposits forming saline mudflats and pans are depicted around a small playa lake. Model B indicates more humid conditions than model A, smaller straight crested dunes are present with larger interconnected flooded interdune areas. A large desert lake is shown in front of the model.

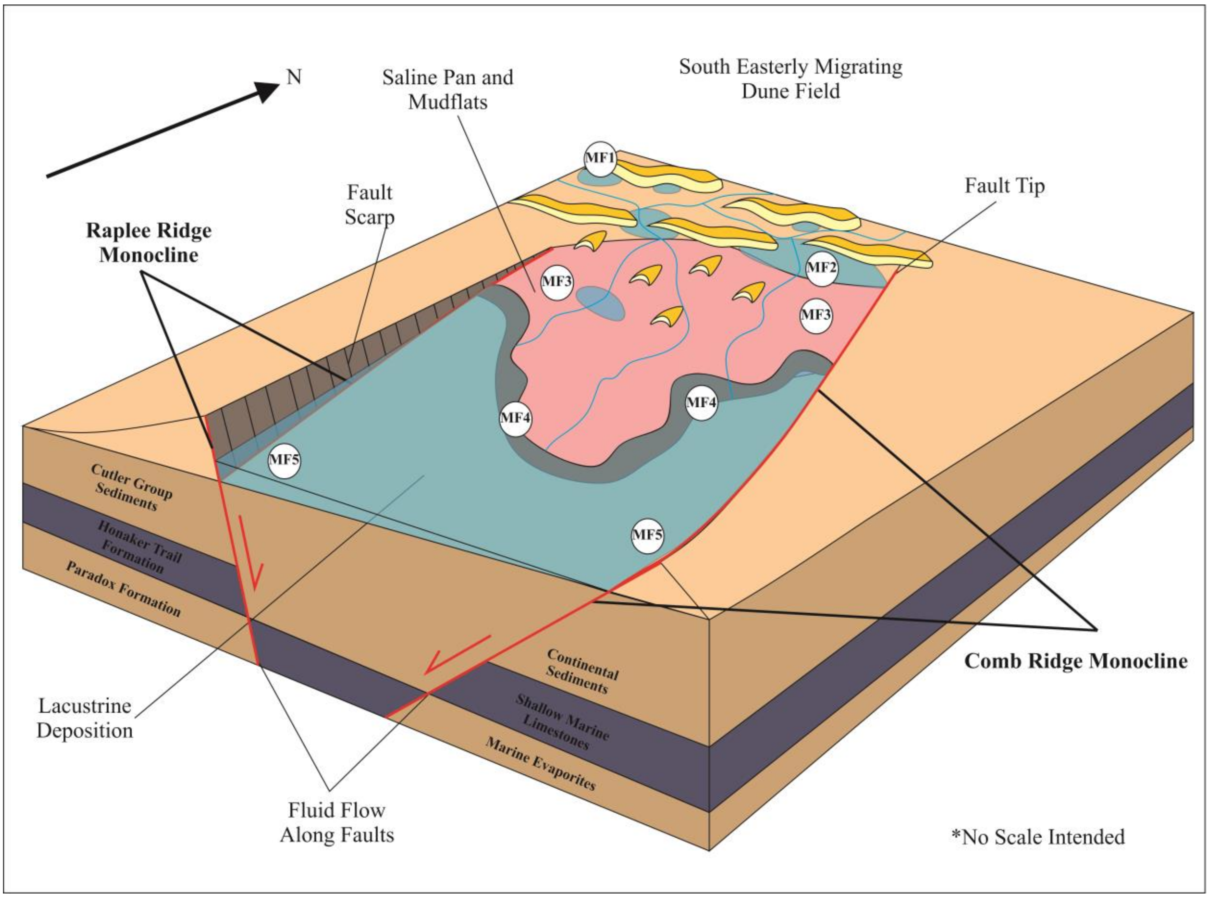

Figure 12 Schematic depositional model depicting the possible role that fault generated topography played on the arrangement and deposition of facies of the Cedar Mesa Sandstone Formation. The faults are shown in red with the interpreted depositional environments between. The location of each microfacies are marked with white circles, and the number of the microfacies within. The sabkha environment is shown in pink, lacustrine environment in blue, dunes are drawn in yellow.